[AMERICAN JOURNAL OF SCIENCE, SCHAIRER VOL. 267-A, 1969, P 295-324]

SUBSOLIDUS RELATIONS ALONG THE JOIN HEDENBERGITE-FERROSILITE

D. H. LINDSLEY and J. L. MUNOZ

Geophysical Laboratory,
Carnegie Institution of Washington,
Washington, D.C. 20008

ABSTRACT. An investigation of the subsolidus relations along the join hedenbergite ($Ca_{0.50}Fe_{0.50}SiO_3$)–ferrosilite ($FeSiO_3$) under a variety of conditions has shown the following:

1. At low pressures (at and below 2 kb) hedenbergitic clinopyroxenes on this join are stable over the compositional range from $Ca_{0.50}Fe_{0.50}SiO_3$ to a maximum Fe-content of $Ca_{0.40}Fe_{0.60}SiO_3$; the latter corresponds closely to the compositions of the latest clinopyroxenes to crystallize from the Skaergaard and Bushveld intrusions. More iron-rich compositions on the join are represented by the three-phase assemblages hedenbergite$_{ss}$ + fayalite + SiO_2 (below 940°C) and Fe-wollastonite$_{ss}$ + fayalite + SiO_2 (above 940°C).

2. Pyroxenes are not stable at low pressures (at and below 2 kb) in a zone of the pyroxene quadrilateral that extends from the ferrosilite apex about to $Ca_{0.40}Fe_{0.60}SiO_3$ along the hedenbergite–ferrosilite join and approximately to $Mg_{0.15}Fe_{0.85}SiO_3$ along the enstatite-ferrosilite join. This portion of the quadrilateral is termed the "forbidden zone" to emphasize the instability of pyroxenes within it at low pressures; bulk compositions within this zone are represented by the assemblage fayalite + silica with or without Ca-rich pyroxene. For this reason, compositional trends of Ca-poor pyroxenes from crustal rocks cannot extend to the hedenbergite-ferrosilite join.

3. At 20 kb a two-pyroxene assemblage is stable on the hedenbergite-ferrosilite join: orthopyroxene (approximately $Ca_{0.05}Fe_{0.95}SiO_3$) and clinopyroxene ($Ca_{0.36}Fe_{0.64}SiO_3$ at 800°C; $Ca_{0.08}Fe_{0.92}SiO_3$ at 950°C); the range of clinopyroxene compositions is extremely temperature-dependent at this high pressure. Extrapolation of the high-pressure relations to low pressures suggests the existence of a *metastable* two-pyroxene field within the "forbidden zone" of the quadrilateral; the extrapolated two-pyroxene field on the hedenbergite-ferrosilite join thus serves as a probable (metastable) terminus of the two-pyroxene field of the pyroxene quadrilateral.

4. The cessation of crystallization of Ca-poor pyroxenes and the concomitant minimum in the Ca/(Ca + Mg + Fe) ratio of the coexisting Ca-rich pyroxenes in the Bushveld and Skaergaard intrusions probably is a function of the silica activity in each magma. The absence of quartz as a primary phase during the intermediate stages of fractionation in these bodies precludes the alternative interpretation that these features reflect a reaction: clinopyroxene + orthopyroxene + liquid = clinopyroxene + olivine + quartz + liquid.

5. A previously reported stability field of clinoferrosilite below 800°C is now shown to be shear-sensitive; in the absence of shearing stresses (under hydrothermal conditions) at 20 kb orthoferrosilite appears to be the only stable polymorph of $FeSiO_3$ below about 1100°C. Hydrothermal experiments at 100 bars show that orthoferrosilite inverts to clinoferrosilite at temperatures of 900°C and above, even while both polymorphs are breaking down to the stable assemblage fayalite + tridymite. This result, although unconfirmed by reversed reaction, provides a probable upper temperature limit for the iron-rich end of the hypersthene-pigeonite transition loop.

INTRODUCTION

The compositions of pyroxenes from a large number of igneous rocks can be plotted for the most part in the "pyroxene quadrilateral", the reciprocal system diopside ($Ca_{0.50}Mg_{0.50}SiO_3$, Di)–hedenbergite ($Ca_{0.50}Fe_{0.50}SiO_3$, Hd)–enstatite ($MgSiO_3$, En)–ferrosilite ($FeSiO_3$, Fs). The phase relations of pyroxenes within this system can therefore provide a great deal of information on the crystallization histories of those rocks. No man has done more than J. Frank Schairer to elucidate these phase

relations, and in the knowledge that his many contributions have made this paper possible we gratefully dedicate it to him.

Because the pyroxenes of many volcanic rocks may have crystallized out of equilibrium, they will not be considered in this discussion. In hypabyssal and plutonic igenous rocks there are three main groups of pyroxenes with compositions that can be plotted in the pyroxene quadrilateral: (1) a complete series of clinopyroxenes with space group $C\ 2/c$ ranging in composition from diopside through augite to hedenbergite; (2) a series of orthopyroxenes with space group Pbca and with compositons lying close to the enstatite-ferrosilite join; and (3) a series of clinopyroxenes (pigeonites) with space group $P\ 2_1/c$ whose compositions (plotted according to the method of Hess, 1949) lie on a trend-line parallel to the enstatite-ferrosilite join but which contain about 9 mole percent $CaSiO_3$. Some orthopyroxenes containing exsolved lamellae of augite have the bulk compositions of pigeonites and are believed to have inverted from pigeonites. In this paper, orthopyroxenes and pigeonites will be classed together as Ca-poor pyroxenes, and the diopside–augite–hedenbergite series will be referred to as Ca-rich pyroxenes. Many plutonic and hypabyssal pyroxenes contain exsolution lamellae; the discussion here will deal with the bulk compositions of these intergrowths, since presumably they crystallized as single phases.

The pyroxenes of strongly differentiated gabbroic bodies commonly show a wide range of compositions, the Fe/Mg ratios of both Ca-poor and Ca-rich varieties increasing during fractionation (and hence with decreasing temperature of the magma). The trends of pyroxene compositions for the Bushveld and Skaergaard intrusions are shown in figure 1. Several features of these trends are germane to this paper: (1) In the earlier crystallization stages of each body Ca-rich and Ca-poor pyroxenes co-precipitated; but with advanced fractionation, Ca-poor pyroxenes ceased to crystallize. (2) The Ca-rich trends tend to converge toward the Ca-poor trends with increasing Fe/Mg ratio (and hence with falling temperature of the differentiating magma). (3) The Ca-rich pyroxenes form continuous trends from near the Di-En join to the Hd-Fs join, trends for both bodies ending at virtually identical compositions. (4) In each body the Ca-rich trend passes through a minimum in calcium content with increasing Fe/Mg ratio. Each calcium minimum, which lies at a different Fe/Mg ratio on each trend-line, is shown by that Ca-rich pyroxene in equilibrium with the last Ca-poor pyroxene to crystallize. The Ca-rich trends are nearly coincident at either end; they diverge significantly only in the vicinity of the calcium minimum in the Bushveld trend.

Much experimental work on the pyroxene quadrilateral has been directed at explaining relations of natural pyroxenes. In their study of melting relations in the pyroxene quadrilateral, Yoder, Tilley, and Schairer (1963, 1964) discovered many of the principles that govern the crystallization of pyroxenes from a fractionating liquid. Because of the abundance of additional components (Al_2O_3, Fe_2O_3, Na_2O, et cetera) in magmas, however, natural liquids will generally precipitate a pyroxene

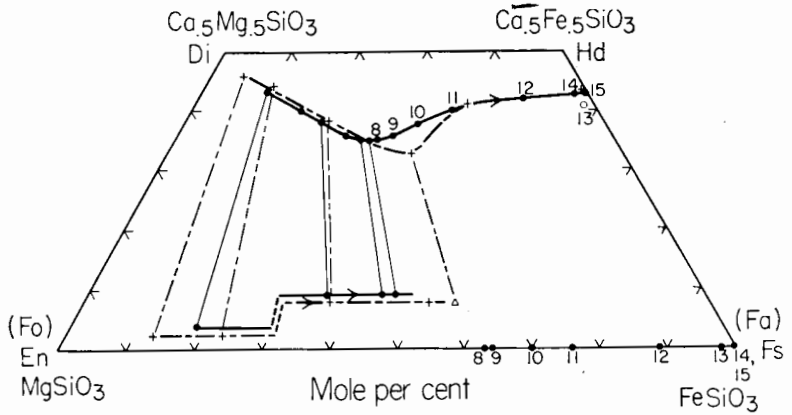

Fig. 1. Trends of pyroxene compositions for the Skaergaard and Bushveld intrusions. Skaergaard: solid circles, compositions of analyzed pyroxenes; open circle, composition of analyzed inverted ferriferous wollastonite; heavy solid lines, trends of Ca-rich and Ca-poor pyroxenes; light solid lines, tie lines between coexisting pyroxenes (Brown, 1957; Brown and Vincent, 1963). Dots along Fs-En join give Fe/Mg ratios of olivines coexisting with similarly-numbered Ca-rich pyroxenes from the Skaergaard intrusion. Bushveld: crosses, analyzed pyroxenes; triangle, composition of latest cumulus Ca-poor pyroxene (optical determination); heavy dash-dot lines, trends of Ca-rich and Ca-poor pyroxenes; light dash-dot lines, tie lines between coexisting pyroxenes (Atkins, quoted in Wager and Brown, 1968). Dashed lines, compositional breaks between orthopyroxenes and pigeonites. Arrows show direction of progressive crystallization.

of a given Fe/Mg ratio at a lower temperature than is found for bulk compositions lying essentially in the pyroxene quadrilateral. (The additional components will also enter the pyroxene, of course, but in much smaller proportions than in the coexisting liquid.) Thus while the results of Yoder, Tilley, and Schairer provide important insights into the mechanisms of pyroxene crystallization, they should be applied to magmas with some caution.

An alternative approach to the study of pyroxene relations—an approach that must ultimately be complementary to and consistent with that of Yoder, Tilley, and Schairer—is to assume that the *subsolidus* relations in the pyroxene quadrilateral are not significantly changed by small differences in the tenor of minor constitutents. (Analyzed pyroxenes from the Skaergaard intrusion contain at least 91 percent $CaSiO_3$ + $MgSiO_3$ + $FeSiO_3$ (Brown, 1957; Brown and Vincent, 1963).) To the extent that this assumption is valid, the subsolidus relations of synthetic pyroxenes should be closely similar to those of natural pyroxenes. Thus if we knew the subsolidus relations of the pyroxenes, we could view different magmas as intersecting those relations over different temperature intervals characteristic of those magmas. For example, if we knew the width of a two-pyroxene field as a function of temperature, we might determine which of two magmas attained a given stage of fractionation at the lower temperature. We have adopted this approach, using data on synthetic systems for the subsolidus relations on the bounding joins

and using the compositions of analyzed natural pyroxenes to extrapolate into the quadrilateral. Eventually, of course, our extrapolation must be checked by direct experimental determination of subsolidus relations of natural and synthetic pyroxenes lying within the quadrilateral. A drawback of our approach is that it provides no direct information on liquid lines of descent; however, it does provide limitations on the compositions of natural pyroxenes that are largely independent of the presence of other phases and of the composition of the magma. For example, Atlas (1952) and Boyd and Schairer (1964) demonstrated the existence of a two-pyroxene field in the join Di-En. The two-pyroxene fields observed for the Skaergaard and Bushveld intrusions (fig. 1) result from the intersection of a two-pyroxene volume in the quadrilateral with the temperature range of differentiating magma.

Few igneous pyroxenes attain compositions lying on the join hedenbergite-ferrosilite; nevertheless we have investigated that join under a variety of conditions in an attempt to elucidate the subsolidus relations in the Mg-poor portions of the pyroxene quadrilateral.

Previous work on the join Hd-Fs.—The report on the system CaO–FeO–SiO_2 by Bowen, Schairer, and Posnjak (1933) was a landmark in the study of synthetic pyroxenes. Among their important discoveries along the join Hd-Fs (fig. 2) were: (1) Hedenbergitic pyroxenes (henceforth abbreviated as Hd_{ss}) invert to ferriferous wollastonite solid solutions (Wo_{ss}) upon heating to temperatures well below the solidus. Certain hedenbergites in the Skaergaard intrusion are interpreted as having inverted from Wo_{ss} on cooling (Wager and Deer, 1939, p. 111; Brown and Vincent, 1963). (2) The assemblage fayalite + tridymite is stable relative to ferrosilite at 1 atm, thus explaining the absence or rarity of $FeSiO_3$-rich pyroxenes.

Bowen, Schairer, and Posnjak reported that the compositions of Hd_{ss} in equilibrium with the assemblage fayalite + tridymite lie approximately midway between $Ca_{0.50}Fe_{0.50}SiO_3$ and $FeSiO_3$, or approximately at $Fs_{75}Wo_{25}$ (mole percent). In contrast Hd_{ss} which coexists with fayalite + quartz in the Skaergaard and Bushveld intrusions falls much closer to hedenbergite: $Wo_{42.5}En_{0.4}Fs_{57.1}$ (Skaergaard) and $Wo_{42.7}En_{0.5}Fs_{56.8}$ (Bushveld) (see fig. 1).

Ernst (1966, p. 48) found that Hd_{ss} synthesized hydrothermally at 440° to 687°C and 500 to 3000 bars together with fayalite, and quartz had compositions that are inconsistent with both the Bowen-Schairer-Posnjak results and the compositions of the natural hedenbergites. Ernst emphasized that his synthesis experiments might not reflect stable equilibrium.

Redetermination of subsolidus relations for the join Hd-Fs at low pressures.—Limitations on the control of temperature and the inert atmosphere in the apparatus employed by Bowen, Schairer, and Posnjak precluded experiments of more than 48 hours' duration. We have redetermined subsolidus relations for the join Hd-Fs using run durations of up to 40 days for dry experiments above 1000°C and using water as a

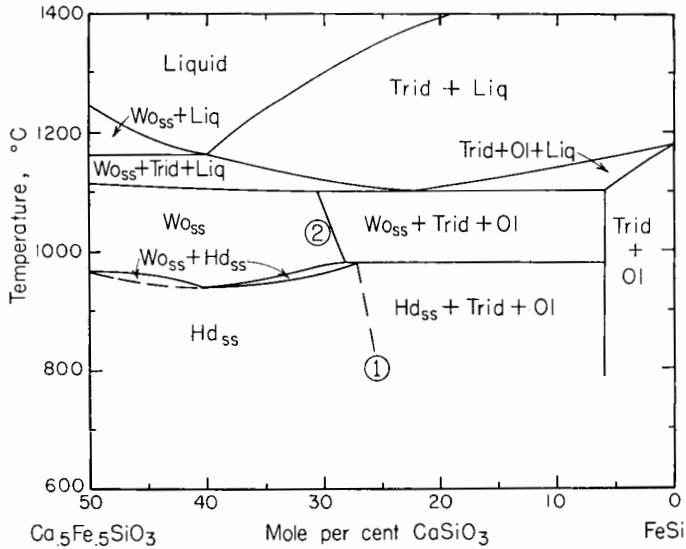

Fig.2. The join hedenbergite-ferrosilite at 1 atm, after Bowen, Schairer, and Posnjak (1933, fig. 8). The liquids contain a small amount of Fe_2O_3. All phases are in equilibrium with metallic iron. Note the minimum in the inversion loop for Hd_{ss}-Wo_{ss}. Curves (1) and (2) are discussed in the text. Liq, liquid; trid, tridymite; Fay, Fe_2SiO_4-rich olivine; Wo_{ss}, Fe-wollastonite solid solutions; Hd_{ss}, hedenbergite solid solutions.

flux at lower temperatures. Our results (table 1) indicate that their subsolidus experiments did not reach equilibrium in 48 hours.

The compositions of Hd_{ss} and Wo_{ss} each in equilibrium with fayalite + SiO_2 (tridymite or quartz) are controlled by the reactions:

$$\text{Fs-rich } Hd_{ss} = \text{Fs-poor } Hd_{ss} + \text{fayalite} + SiO_2 \qquad (1)$$

$$\text{Fs-rich } Wo_{ss} = \text{Fs-poor } Wo_{ss} + \text{fayalite} + SiO_2 \qquad (2)$$

Curves giving the compositions of Hd_{ss} and Wo_{ss} as controlled by these reactions are labelled (1) and (2) in figure 2. These reactions do not involve redox reactions and are independent of oxygen fugacity (fO_2) within the range of fO_2 where the individual phases remain stable. In essence this range is bounded by the breakdown of fayalite:

$$Fe_2SiO_4 = 2Fe + SiO_2 + O_2$$

and

$$3Fe_2SiO_4 + O_2 = 2Fe_3O_4 + 3SiO_2$$

These are respectively the fayalite–iron–quartz (FIQ) and fayalite–magnetite–quartz (FMQ) buffers (Eugster and Wones, 1962, p. 87-91). Experiments in equilibrium with metallic iron—such as those of Bowen, Schairer, and Posnjak, and our evacuated, silica-tube experiments—are essentially conducted at the FIQ buffer[1]. Most of our hydrothermal ex-

[1] The fO_2 of the FIQ buffer is attained in a system in which the activities of fayalite, iron, and silica are all unity. The activity of iron is unity by design of the experiment, and the activities of fayalite and tridymite are unity or nearly so over much of the Hd-Fs join.

TABLE 1

Determinative experiments at and below 2000 bars on the join hedenbergite-ferrosilite

Starting material phases (bulk composition)	Temp., ±5°C	Pressure, ±20 bars	Buffer	Duration		Results
				Days	Hours	
Cpx ($Fs_{60}Wo_{40}$)	950	500	FMQ		4-1/2	Hd_{ss} (+ minor Wo_{ss})
Cpx ($Fs_{60}Wo_{40}$)	955	500	FMQ		4	Hd_{ss} + Wo_{ss}
Cpx ($Fs_{60}Wo_{40}$)	960	500	FMQ		7-1/2	Hd_{ss} + Wo_{ss}
Cpx ($Fs_{60}Wo_{40}$)	965	500	FMQ		7-1/2	Wo_{ss} (+ minor Hd_{ss})
Cpx ($Fs_{60}Wo_{40}$)	1000	(evac)	(Fe)	40	0	Wo_{ss}
Wo_{ss} ($Fs_{60}Wo_{40}$)	950	500	FMQ		11	Wo_{ss} (+ minor Hd_{ss})
Hd + Fay + Qtz ($Fs_{65}Wo_{35}$)	600	2000	FMQ	55	0	Hd_{ss} ($Fs_{54.5\pm2}$) + Fay + Qtz (+ Mt)
Hd + Fay + Qtz ($Fs_{65}Wo_{35}$)	700	1000	WM	34	19	Hd_{ss} ($Fs_{56.5\pm2}$) + Fay + Qtz
Hd + Fay + Qtz ($Fs_{65}Wo_{35}$)	800	2000	FMQ	6	0	Hd_{ss} ($Fs_{55.5}$) + Fay + Qtz
Hd + Fay + Qtz ($Fs_{65}Wo_{35}$)	850	2000	FMQ	2	20	Hd_{ss} (Fs_{57}) + Fay + Qtz
Hd + Fay + Qtz ($Fs_{65}Wo_{35}$)	900	2000	FMQ		18	Hd_{ss} (Fs_{58}) + Fay + Qtz
Hd + Wo_{ss} + Fay + Qtz ($Fs_{65}Wo_{35}$)	965	140	FMQ	2	21	Wo_{ss} ($Fs_{61.5}$) + Fay + Trid
Hd + Wo_{ss} + Fay + Qtz ($Fs_{65}Wo_{35}$)	980	230	FMQ		19	Wo_{ss} ($Fs_{61.5}$) + Fay + Trid
Hd + Wo_{ss} + Fay + Qtz ($Fs_{65}Wo_{35}$)	1000	(evac)	(Fe)	40	0	Wo_{ss} ($Fs_{62.5}$) + Fay + Trid
Hd + Wo_{ss} + Fay + Qtz ($Fs_{65}Wo_{35}$)	1080	(evac)	(Fe)	12	19	Wo_{ss} (Fs_{64}) + Fay + Trid
Cpx ($Fs_{65}Wo_{35}$)	1000	(evac)	(Fe)	40	0	Wo_{ss} + Fay + Trid
Wo_{ss} ($Fs_{65}Wo_{35}$)	970	210	FMQ	1	23	Wo_{ss} ($Fs_{63.5}$) + Fay + Trid
Wo_{ss} ($Fs_{65}Wo_{35}$)	1000	225	FMQ		12	Wo_{ss} (Fs_{64}) + Fay + Trid
Wo_{ss} ($Fs_{65}Wo_{35}$)	1080	(evac)	(Fe)	12	19	Wo_{ss} (Fs_{63}) + Fay + Trid
Cpx ($Fs_{70}Wo_{30}$)	600	2000	FMQ	51	22	Hd_{ss} ($Fs_{56.5}$) + Fay + Qtz
Cpx ($Fs_{70}Wo_{30}$)	800	1000	WM	3	21	Hd_{ss} (Fs_{58}) + Fay + Qtz (+ Mt)
Cpx ($Fs_{70}Wo_{30}$)	800	1000	FMQ	5	16	Hd_{ss} ($Fs_{61.5}$) + Fay + Qtz
Cpx ($Fs_{70}Wo_{30}$)	825	2000	FMQ	2	16	Hd_{ss} ($Fs_{59.5}$) + Fay + Qtz
Cpx ($Fs_{70}Wo_{30}$)	900	2000	FMQ		8	Hd_{ss} ($Fs_{60.5}$) + Fay + Qtz
Cpx ($Fs_{70}Wo_{30}$)	975	500	FMQ		4	Wo_{ss} + Fay + Trid
Cpx ($Fs_{70}Wo_{30}$)	1000	(evac)	(Fe)	40	0	Wo_{ss} + Fay + Trid
Wo_{ss} ($Fs_{70}Wo_{30}$)	1080	(evac)	(Fe)	13	0	Wo_{ss} (Fs_{62}) + Fay + Trid
Wo_{ss} ($Fs_{70}Wo_{30}$)	965	140	FMQ	2	21	Wo_{ss} ($Fs_{65.5}$) + Fay + Trid
Hd + Fay + Qtz ($Fs_{75}Wo_{25}$)	650	2000	FMQ	38	23	Hd_{ss} ($Fs_{52.5}$) + Fay + Qtz
Hd + Fay + Qtz ($Fs_{75}Wo_{25}$)	700	2000	FMQ	62	0	Hd_{ss} ($Fs_{56\pm2}$) + Fay + Qtz

TABLE 1 (continued)

Starting material phases (bulk composition)	Temp., ±5°C	Pressure, ±20 bars	Buffer	Duration		Results
				Days	Hours	
Cpx ($Fs_{75}Wo_{25}$)	630	2000	FMQ	27	15	Hd_{ss} ($Fs_{55}\pm2$) + Fay + Qtz (+ Mt)
Cpx ($Fs_{80}Wo_{20}$)	780	2000	WM		23	Hd_{ss} (Fs_{61}) + Fay + Qtz
Cpx ($Fs_{80}Wo_{20}$)	780	2000	FMQ	3	17	Hd_{ss} (Fs_{59}) + Fay + Qtz
Cpx ($Fs_{80}Wo_{20}$)	850	1000	WM		10-1/2	Hd_{ss} ($Fs_{61.5}$) + Fay + Qtz
Cpx ($Fs_{80}Wo_{20}$)	850	1000	FMQ	1	0	Hd_{ss} ($Fs_{61.5}$) + Fay + Qtz
Cpx ($Fs_{80}Wo_{20}$)	900	1000	WM		8	Hd_{ss} (Fs_{63}) + Fay + Qtz
Cpx ($Fs_{90}Wo_{10}$)	940	400	FMQ	3	0	Hd_{ss} ($Fs_{60}\pm2$) + Fay + Qtz

Abbreviations:

Cpx, clinopyroxenes with compositions between $CaFeSi_2O_6$ and $FeSiO_3$.
Hd, $CaFeSi_2O_6$.
Hd_{ss}, clinopyroxenes close to $CaFeSi_2O_6$ in composition.
Wo_{ss}, Fe-wollastonite solid solutions (composition $CaFeSi_2O_6$ for starting material, between $CaFeSi_2O_6$ and $FeSiO_3$ for run products).
Fay, olivine close to Fe_2SiO_4.
Qtz, quartz.
Trid, tridymite.
Mt, magnetite.

Oxygen buffers:

FMQ, fayalite + magnetite + SiO_2 (quartz or tridymite, depending on pressure and temperature).
WM, wüstite + magnetite.
(Fe), evacuated tube experiments, sample enclosed in iron capsule, with oxygen fugacity close to that of the fayalite + iron + quartz buffer.

Compositions of metasilicates in run products are expressed in mole percentages of $FeSiO_3$ (Fs) in $CaSiO_3$ (Wo) and are ±1 percent unless otherwise stated.

periments employed the FMQ buffer. However, we would emphasize that there should be no effect on reactions (1) and (2) due to the different oxygen fugacities in these sets of experiments. Reactions (1) and (2) are indifferent to the presence of metallic iron or of magnetite so long as the assemblage fayalite + SiO_2 is present. Ernst (1966, p. 45-48) found no differences between Hd_{ss} synthesized at iron-magetite, wüstite-magnetite, and fayalite-magnetite-quartz buffers, but Hd_{ss} synthesized at the nickel–nickel oxide buffer (which lies outside the fayalite stability field) did vary significantly from those compositions. In the latter case, reaction (1) must be replaced by a redox reaction. We have used buffers in our hydrothermal experiments at and below 2 kb, not because oxygen takes part in reactions (1) and (2), but because in standard hydrothermal apparatus it is otherwise impossible to prevent oxidation of the sample. The equilibria of reactions (1) and (2) are independent of the presence of an aqueous vapor phase unless one of the solid phases dissolves completely in the vapor or H_2O enters one of the solid phases; neither of these conditions occurs in our experiments. The water in our hydrothermal experiments serves only as a pressure medium and as a catalyst to increase reaction rates. Reactions (1) and (2) are pressure-sensitive (compare, Lindsley, 1967), but we found no detectable effect at pressures ranging from 200 to 2000 bars.

For the most part we have used as starting materials only those phases that take part in the reaction being studied, so that our results reflect reversed equilibrium, evidently stable equilibrium, rather than synthesis. An exception to this rule is silica: we have found that silica polymorphs invert in much shorter time than is required for Hd_{ss} to change composition, so that it is immaterial in determining reactions (1) and (2) what polymorph of silica is used. Details on experimental techniques and the preparation of starting materials are given in the Appendix. All compositions of synthetic Ca-Fe pyroxenes and pyroxenoids are given in mole percent $FeSiO_3$ (Fs) and $CaSiO_3$ (Wo).

Results of experiments that determine the compositions of Hd_{ss} and Wo_{ss} in equilibrium with fayalite + quartz are given in table 1 and summarized in figure 3A. Data on Hd_{ss} were obtained at temperatures from 600° to 940°C and at water pressures from 400 to 2000 bars. Data on Wo_{ss} were obtained at 140 to 500 bars water pressure below 1000°C and *in vacuo* at and above 1000°C.

Curves (1) and (2) of figure 2 given by Bowen, Schairer, and Posnjak lie well within the three-phase fields defined by reversed reaction in our experiments. Note that our revised curve (fig. 3A) for reaction (1) very nearly intersects the minimum in the Hd_{ss}-Wo_{ss} inversion loop given by Bowen, Schairer, and Posnjak. Our data fit the Hd-rich half of that loop almost perfectly: in experiments at 950°C and 500 bars on the composition $Fs_{60}Wo_{40}$, Hd_{ss} reacts to Hd_{ss} + Wo_{ss}, and Wo_{ss} also reacts to Hd_{ss} + Wo_{ss}; this locates a point in the Wo_{ss} + Hd_{ss} field. We have drawn the inversion loop using the Bowen-Schairer-Posnjak temperature for the inversion of $Ca_{0.50}Fe_{0.50}SiO_3$.

The compositions of Hd_{ss} at 940°C given by our experiments—$Fs_{60\pm2}Wo_{40\pm2}$—are in agreement with the compositions of the latest hedenbergites to crystallize in the Skaergaard and Bushveld intrusions (fig. 1). The composition of Wo_{ss} in equilibrium with fayalite + quartz is about 2 percent richer in $FeSiO_3$, consistent with the composition of the green, mosaic-textured hedenbergite from EG4471 in the Skaergaard intrusion which is believed to have inverted from a wollastonite solid solution (Brown and Vincent, 1963, p. 177, 181, 186-190).

The discrepancy between our results and those of Bowen, Schairer, and Posnjak on the compositions of Hd_{ss} and of Wo_{ss} in equilibrium with fayalite + silica cannot be explained on the basis of different oxygen fugacities (there is no redox reaction) or pressures (the higher pressures in some of our experiments should bias our results, if at all, toward compositions richer rather than poorer in $FeSiO_3$; compare, Lindsley, 1967). The presence of water can affect the reaction only if water enters one or more of the solid phases. However, we have found no difference in the X-ray patterns of hedenbergite solid solutions synthesized dry and hydrothermally as would be expected if water entered the pyroxene structure. (For a counter-example, however, see Sclar, Carrison, and Stewart, 1968.) We can only conclude that the subsolidus results of Bowen, Schairer, and Posnjak reflect incomplete reaction or metastable equilibrium, probably as a result of the short-run durations required by their apparatus. A revised diagram for the join Hd-Fs, incorporating our subsolidus data with the melting relations of Bowen, Schairer, and Posnjak, is given in figure 3B.

Subsolidus relations for the join Hd-Fs at 20 kb.—Curve (1) in figure 3 marks the limit of stable solid solution of $FeSiO_3$ in hedenbergite at low pressures. Bulk compositions lying to the right of curve (1) will crystallize at equilibrium to Hd_{ss} + Fay + SiO_2 or to Fay + SiO_2. Lindsley (1967, p. 234) showed that curve (1) is shifted toward $FeSiO_3$ (that is, the Hd_{ss} field becomes wider) with increasing pressure and concluded (p. 232) that at 1000°C there is complete solid solution between clinoferrosilite and hedenbergite at 20 kb. This interpretation can be schematically illustrated by use of free energy-composition plots (fig. 4, A-C). The free energy for the assemblage Ca-Fe olivine + SiO_2 (1:1 mole ratio) increases relative to that for Ca-Fe Cpx with increasing pressure; as the free-energy curve for Cpx is everywhere convex downward, the field of Cpx widens continuously with increasing pressure.

At lower temperatures (say, 750°C) it is possible that a miscibility gap occurs in the Cpx series. At low pressures this miscibility gap would be masked by the stable assemblage Hd_{ss} + Fay + SiO_2 (fig. 4D). Note that the Hd_{ss} (composition x in fig. 4D) in stable equilibrium with Fay + SiO_2 must always be poorer in $FeSiO_3$ than the Hd_{ss} (composition y) in metastable equilibrium with Fs_{ss} (composition z). (We suggest that Ernst's (1966) synthesis data may give metastable values of y.) Thus curve (1) in figure 3 cannot be one boundary of a miscibility gap, but it is impossible to tell from figure 3 whether there might be a metastable miscibility

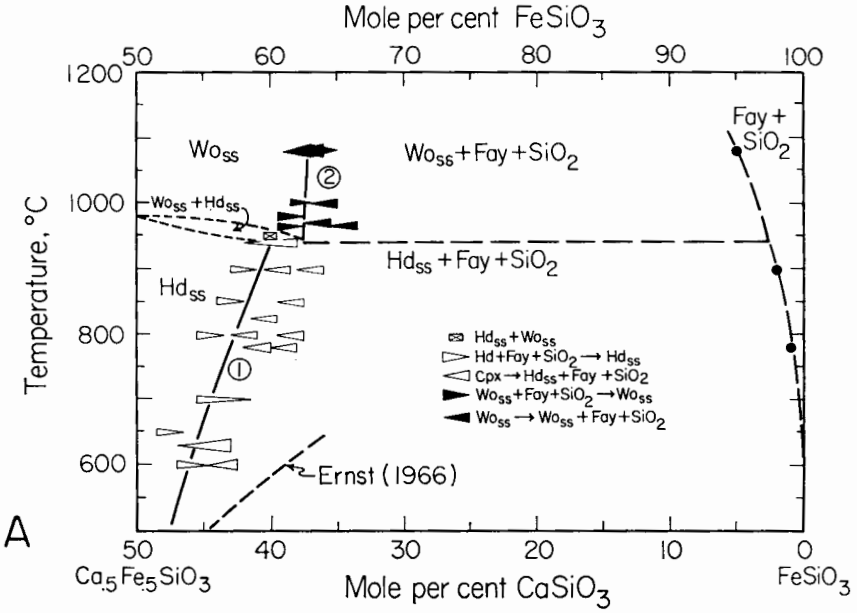
Mole per cent FeSiO3
50
60
70
80
90
100
1200
1000
800
600
Temperature, °C
Wo_ss
Wo_ss + Fay + SiO2
Fay + SiO2
Wo_ss + Hd_ss
Hd_ss + Fay + SiO2
Hd_ss
Hd_ss + Wo_ss
Hd + Fay + SiO2 → Hd_ss
Cpx → Hd_ss + Fay + SiO2
Wo_ss + Fay + SiO2 → Wo_ss
Wo_ss → Wo_ss + Fay + SiO2
Ernst (1966)
A
50
40
30
20
10
0
Ca5Fe5SiO3
Mole per cent CaSiO3
FeSiO3

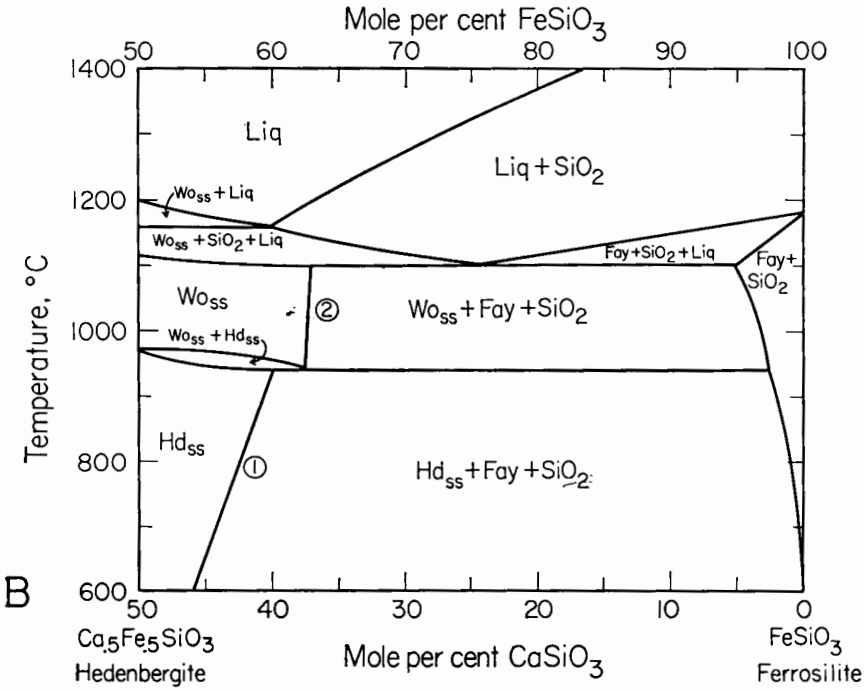
Mole per cent FeSiO3
50
60
70
80
90
100
1400
1200
1000
800
600
Temperature, °C
Liq
Liq + SiO2
Wo_ss + Liq
Wo_ss + SiO2 + Liq
Fay + SiO2 + Liq
Fay + SiO2
Wo_ss
Wo_ss + Fay + SiO2
Wo_ss + Hd_ss
Hd_ss
Hd_ss + Fay + SiO2
B
50
40
30
20
10
0
Ca5Fe5SiO3
Hedenbergite
Mole per cent CaSiO3
FeSiO3
Ferrosilite

gap lying entirely within the stable Hd_{ss} + Fay + SiO_2 field (note the identical sets of assemblages in figs. 4A and D). At 20 kb, however, clinopyroxenes are stable relative to Hd_{ss} + Fay + SiO_2 (fig. 4F), and if a miscibility gap exists, it should appear in a 20 kb temperature-composition diagram. This miscibility gap could be extrapolated to low pressures to provide a metastable terminus for the two-pyroxene field in the pyroxene quadrilateral. (To simplify the free-energy diagrams, we have ignored the possible stability of orthopyroxene in this discussion.)

We have discovered a two-pyroxene field on the join Hd-Fs (fig. 5A; table 2) by employing hydrothermal experiments at 20 kb, a pressure at which ferrosilite is stable (compare, Lindsley, MacGregor, and Davis, 1964). The coexisting pyroxenes are an orthopyroxene (OFs_{ss}) with the approximate composition $Fs_{95}Wo_5$ and a clinopyroxene (Cpx) whose composition varies from about $Fs_{60}Wo_{40}$ at 800°C to $Fs_{92}Wo_8$ at 950°C. The wide range of Cpx compositions above 950°C is consistent with the previous data obtained in dry experiments at high pressures (Lindsley, 1967).

Three kinds of starting materials were employed for the 20 kb hydrothermal experiments. They are (A) single-phase clinopyroxene of bulk compositions $Fs_{75}Wo_{25}$, $Fs_{85}Wo_{15}$, $Fs_{90}Wo_{10}$, and $Fs_{95}Wo_5$; (B) two-phase mixtures of hedenbergite and ortho-ferrosilite with bulk compositions $Fs_{75}Wo_{25}$, $Fs_{90}Wo_{10}$, and $Fs_{95}Wo_5$; and (C) two-phase mixtures of the clinopyroxenes $Fs_{60}Wo_{40}$ and $Fs_{90}Wo_{10}$ with bulk compositions $Fs_{75}Wo_{25}$ and $Fs_{82}Wo_{18}$. By use of appropriate starting materials, the boundaries of the two-pyroxene field have been bracketed by reversed reaction. The curve giving the composition of clinopyroxene in equilibrium with OFs_{ss} is very temperature-sensitive in the range 750° to 900°C (fig. 5A). Near 900°C there is a dramatic increase in the slope of that curve. This change in slope could represent either the presence of an additional pyroxene phase (implying that three pyroxenes—Hd_{ss}, "ferropigeonite," and ortho-ferrosilite—would coexist at the temperature corresponding to the change in slope; fig. 5B) or the interference of two different elements of two-pyroxene equilibria (a miscibility gap in

Fig. 3. The join hedenbergite-ferrosilite at low pressures (at and below 2 kb). Liq, liquid (containing a small amount of Fe_2O_3); Wo_{ss}, Fe-wollastonite solid solutions; Hd_{ss}, clinopyroxene solid solutions close to $Ca_{0.50}Fe_{0.50}SiO_3$ but extending toward $FeSiO_3$; Cpx, clinopyroxenes with compositions between $Ca_{0.50}Fe_{0.50}SiO_3$ and $FeSiO_3$; Fay, olivine close in composition to Fe_2SiO_4; SiO_2, quartz or tridymite, depending on pressure and temperature. Curves (1) and (2) are discussed in the text.

A. Compositions of Hd_{ss} and Wo_{ss} in equilibrium with fayalite + SiO_2, determined at pressures from nearly zero (evacuated tube experiments) to 2 kb water pressure. The uncertainty in temperature and composition for each experiment is represented by an imaginary rectangle circumscribing each triangle. Compositions of fayalites have not been bracketed by reversed reaction and may not represent equilibrium compositions. Temperature of Hd-Wo_{ss} inversion for $Ca_{0.50}Fe_{0.50}O_3$ composition from Bowen, Schairer, and Posnjak (1933). Curve labelled Ernst (1966) is for synthesis of Hd_{ss} coexisting with fayalite + quartz.

B. Revised diagram for the join hedenbergite-ferrosilite. Sub-solidus data from figure 3A. Data above solidus from Bowen, Schairer, and Posnjak (1933), calculated as mole percent; see figure 2, this paper.

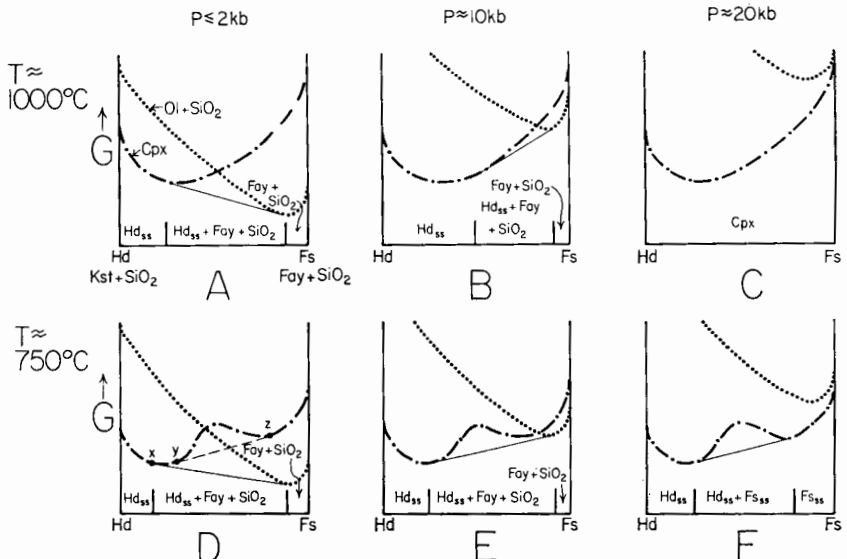

Fig 4. Schematic free energy-composition diagrams plotted as a function of 3 pressures for temperatures of 1000°C and 750°C. Dash-dot lines: free energy for clinopyroxene solid solutions; dotted lines: free energy for equimolar olivine + SiO_2 mixtures. Polymorphism in ferrosilite is not considered. Solid tangent lines connect coexisting stable phases, and dashed tangent line (y-z in D) connects two coexisting metastable clinopyroxenes. The high temperature sections (A-C) show the effect of pressure on increasing the solubility of $FeSiO_3$ in $Ca_{0.5}Fe_{0.50}SiO_3$; at 20 kb there is complete solid solution along the join. At lower temperatures (D-F) a miscibility gap in the clinopyroxene series is assumed to exist. This miscibility gap is metastable at low pressures (D, E) but becomes stable at high pressures (F). From (D) it is obvious that at low pressures the metastable miscibility gap (y-z) must always be to the right of the stable curve defining the composition (x) of Hd_{ss} in equilibrium with Fay + SiO_2. Note that it is impossible to demonstrate the existence of a metastable miscibility gap at low pressures inasmuch as the stable assemblages shown in A and D are identical.

the clinopyroxenes and an orthopyroxene-clinopyroxene transition loop; fig. 5C).

These alternative interpretations correspond to those advanced by Kushiro (1969) for the diopside-enstatite join at 20 kb and by Davis and Boyd (1966, p. 3573) for the same join at 30 kb. In the latter interpretation, a clinopyroxene miscibility gap has penetrated the lower boundary of the Opx-Cpx transition loop and has deformed but not penetrated the upper boundary (fig. 5C). In the former interpretation (fig. 5B) the miscibility gap has penetrated both the lower and upper boundaries of the transition loop.

In view of Kushiro's evidence for the existence of a two-clinopyroxene field on the Di-En join at 20 kb, we have searched carefully for a similar field on the Hd-Fs join but have not found one. Consequently we have adopted the interpretation shown in figure 5C. (We cannot, however, categorically eliminate the possibility that a narrow (< 10 mole percent wide) two-clinopyroxene field might exist on the Hd-Fs join at 20 kb.) At some different pressure the clinopyroxene miscibility gap might well penetrate through the upper boundary of the Opx-Cpx transition loop, yielding a diagram similar to figure 5B.

TABLE 2

Determinative experiments at 20 kb on the join hedenbergite-ferrosilite

Starting material phases (bulk composition)	Temp.*	Time		Results
		Days	Hours	
Cpx ($Fs_{75}Wo_{25}$)**	785 ± 15	27	1	Cpx (Fs_{64}) + Opx (Fs_{96}†)
Hd + Fs ($Fs_{75}Wo_{25}$)**	785 ± 15	27	1	Cpx (Fs_{61}) + Opx (Fs_{97}†)
Hd + Fs ($Fs_{75}Wo_{25}$)**	760 + 15 − 20	27	1	Cpx (Fs_{58}) + Opx (Fs_{96}†)
Cpx ($Fs_{75}Wo_{25}$)**	705 + 30 − 50	27	1	Cpx (Fs_{61}) + Opx (Fs_{97}†)
Cpx ($Fs_{75}Wo_{25}$)	810	12	20	Cpx (Fs_{70}) + Opx + (Fay)
Hd + Fs ($Fs_{75}Wo_{25}$)	885	9	19	Cpx (Fs_{73}) + Opx + (Fay)
Cpx ($Fs_{75}Wo_{25}$)	885	3	19	Cpx (Fs_{75})
Hd + Fs III	885	3	19	Cpx (Fs_{77}) + Opx + (Fay)
2Cpx: $Fs_{90}Wo_{10}$ + $Fs_{60}Wo_{40}$ ($Fs_{75}Wo_{25}$)**	895	6	5	Cpx (Fs_{76})
Cpx ($Fs_{75}Wo_{25}$)**	910	4		Cpx (Fs_{75})
Hd + Fs ($Fs_{75}Wo_{25}$)	910	3	23	Cpx (Fs_{75})
2Cpx: $Fs_{90}Wo_{10}$ + $Fs_{60}Wo_{40}$ ($Fs_{75}Wo_{25}$)**	975	1	20	Cpx (Fs_{75})
2Cpx: $Fs_{90}Wo_{10}$ + $Fs_{60}Wo_{40}$ ($Fs_{82}Wo_{18}$)**	975	5	19	Cpx (Fs_{82}†)
2Cpx: $Fs_{90}Wo_{10}$ + $Fs_{60}Wo_{40}$ ($Fs_{82}Wo_{18}$)**	910	13	17	Cpx (Fs_{82})
Cpx ($Fs_{85}Wo_{15}$)**	835	13	21	Cpx (Fs_{69}) + Opx (Fs_{95}†)
Cpx ($Fs_{85}Wo_{15}$)**	885	7	0	Cpx (Fs_{82}) + Opx
Cpx + Wo_{ss} ($Fs_{85}Wo_{15}$)	910	4	22	Cpx (Fs_{87}, Fs_{85}†) + Opx (Fs_{95}†) + (Fay)
Hd + Fs ($Fs_{90}Wo_{10}$)**	935	3	19	Cpx (Fs_{87}†) + Opx (Fs_{96}†)
Hd + Fs ($Fs_{90}Wo_{10}$)**	985	3	18	Cpx (Fs_{92}†) + Opx (Fs_{96}†)
Hd + Fs ($Fs_{90}Wo_{10}$)**	1010		16	Cpx (Fs_{90})
Cpx ($Fs_{95}Wo_{5}$)**	910	1	21	Cpx + Opx (Fs_{95}†)
Cpx ($Fs_{95}Wo_{5}$)**	985	1	19	Opx crystals with clino overgrowths
Cpx ($Fs_{95}Wo_{5}$)**	1010		16	Opx with clino overgrowths + trace free clino
Cpx ($Fs_{95}Wo_{5}$)††	1110		24	Cpx + Wo_{ss}

Parentheses indicate compositions of Cpx determined by X-ray methods.

*Temperature ±10°C unless otherwise noted. The first four experiments in this table were run simultaneously. The capsules were distributed axially in the same furnace cell. The boundary between the first and second capsule coincided with the broad thermal maximum, and thus their temperature is rather well known. The third and fourth capsules were situated on the continuously steepening end of the thermal gradient, and thus their temperatures are less well known. A map of the thermal gradient for this particular experiment was made with a series of replicate thermal probes. The distances between three junctions of triple-headed thermocouples were designed to correspond to the distances between centers of capsules in the "piggyback" run.

**Bulk compositions contained up to 5 percent excess SiO_2 to saturate the gas phase with respect to silica; quartz is not reported as a run product in these cases.

†Compositions determined by electron probe.

††A "dry" experiment in an iron capsule; all other runs are hydrothermal.

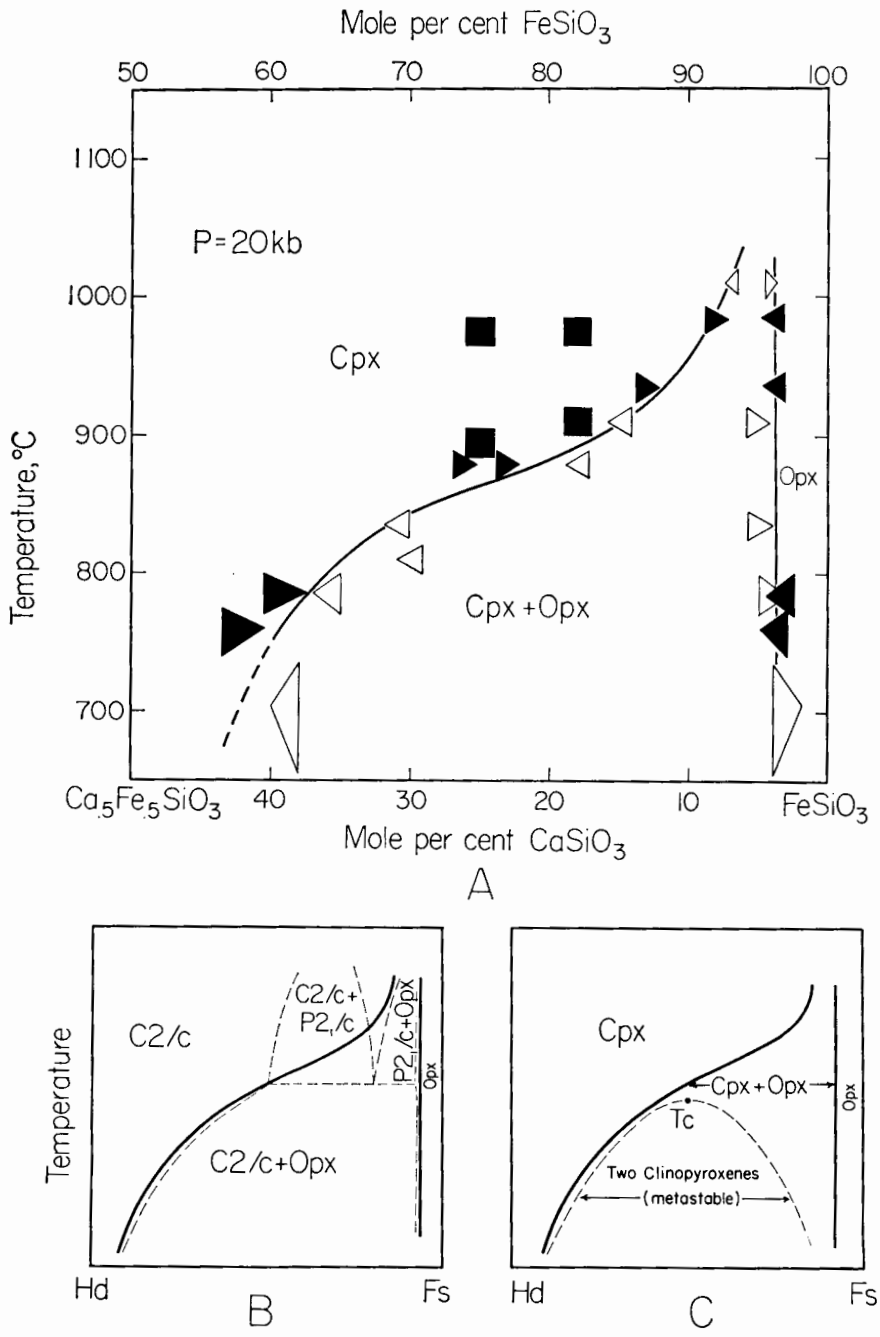
Mole per cent $FeSiO_3$
50
60
70
80
90
100
1100
1000
900
800
700
Temperature, °C
P=20kb
Cpx
Opx
Cpx+Opx
$Ca_5Fe_5SiO_3$
40
30
20
10
$FeSiO_3$
Mole per cent $CaSiO_3$
A
C2/c
C2/c+
P2₁/c
P2₁/c+Opx
Opx
C2/c+Opx
Temperature
Hd
Fs
B
Cpx
Cpx+Opx
Tc
Two Clinopyroxenes
(metastable)
Opx
Hd
Fs
C

Inherent in our interpretation of the 20 kb results is the assumption that there is no first-order transition between Ca-rich and Ca-poor pyroxenes at high temperatures. Natural pigeonites rarely contain more than about 9 percent $CaSiO_3$; however, Burnham (personal commun., 1968) has shown by single-crystal analysis that one of our synthetic clinopyroxenes containing 15 percent $CaSiO_3$ ($Fs_{85}Wo_{15}$) has the pigeonite structure. Single-crystal studies on still more Ca-rich clinopyroxenes will further test this assumption.

ORTHO-PYROXENE-CLINO-PYROXENE INVERSION IN $FeSiO_3$

OFs_{ss} is the only polymorph of ferrosilite observed in all our 20 kb hydrothermal experiments on the Hd-Fs join, including those at temperatures below 800°C (fig. 5A; table 2). Lindsley (1965) described a reversible transition clinoferrosilite (ClFs) $\rightleftarrows$ orthoferrosilite (OFs) at around 800°C. ClFs was reported as the low-temperature form, and, because of the very small $\Delta V_{reaction}$, the inversion is almost insensitive to pressure. However, shearing is known to extend the stability field of monoclinic enstatite (Riecker and Rooney, 1967; Munoz, 1968). Analogously, we have converted OFs to ClFs in an opposed-anvil shearing squeezer (described by Bell and England, 1967) at 900°C and a nominal pressure of 10 kb. By contrast, in the shear-free, hydrothermal environment of our run capsules, we have converted ClFs to OFs at 650°C, or 150°C below the "equilibrium" curve determined under dry conditions (table 3).

Munoz (1968) has demonstrated that a dry sample in piston-and-cylinder apparatus is subjected to somewhat shearing rather than truly hydrostatic conditions. The discrepancy between the data for ferrosilite obtained under dry and under hydrothermal conditions can be explained only if either shearing stress or water (entering the structure of OFs)

Fig. 5. A. Phase relations for the join hedenbergite-ferrosilite at 20 kb. The blunt, vertical edge of each triangle shows the direction from which equilibrium was approached, and the position of each triangle represents the final composition of pyroxene obtained. The size of an imaginary rectangle enclosing each triangle would represent the estimated uncertainties both in temperature and in determination of pyroxene composition. Open triangles within the two-pyroxene field represent single-phase Cpx that broke down to two pyroxenes. Shaded triangles outside the two-pyroxene field show reaction of a two-phase mixture of Hd + Fs. Squares show compositions of homogenized mixtures of two clinopyroxenes, $Fs_{60}Wo_{40}$ + $Fs_{90}Wo_{10}$. Fs, $FeSiO_3$; Hd, $Ca_{0.50}Fe_{0.50}SiO_3$; Cpx, clinopyroxene; Opx, orthopyroxene.

B, C. Schematic interpretations of the two-pyroxene field found at 20 kb on the join Hd-Fs (fig. 5A). Cpx, clinopyroxene with either $C2/c$ or $P2_1/c$ space group; $C2/c$, $P2_1/c$, clinopyroxene with a specific space group. Opx, orthoferrosilite solid solutions. Heavy lines, experimentally determined boundaries of two-pyroxene field. Light curves, elements of equilibrium that might yield the observed diagram.

B. Intersection of three two-phase regions along an isothermal, three-phase line. We have not observed a two-clinopyroxene field ($C2/c$ + $P2_1/c$), but if the field were narrower than shown, its existence might escape detection by X-ray powder diffraction. Our experimental data are probably sufficiently good to preclude the three-phase isothermal element shown.

C. Interference of two elements of two-phase equilibria: a miscibility gap in the clinopyroxene series and a Cpx-Opx transition loop. This interpretation assumes a continuous shift from $C2/c$ (Ca-rich) to $P2_1/c$ (Ca-poor) clinopyroxenes at temperatures above about 900°C. Tc is the critical temperature (870°C) of the assumed miscibility gap. This is our preferred interpretation.

can displace the equilibrium boundary. Although we cannot disprove the latter possibility, we see no optical or X-ray evidence that OFs produced under hydrothermal conditions differs from that produced dry. We therefore suggest that ClFs cannot form at low temperatures in a shear-free environment.

The Cpx + Opx field on the Hd-Fs join at 20 kb (fig. 5A) is terminated in hydrothermal experiments by the appearance of liquid at temperatures above 1010°C and in dry experiments by the appearance of a pyroxenoid at temperatures above 1085° ± 15°C. We anticipate that, if it were not for the advent of these superposing reactions at increasing temperature, the Cpx-Opx transition loop would ultimately terminate at a Cpx-Opx inversion temperature for pure $FeSiO_3$, Cpx being stable at higher and Opx being stable at lower temperatures. The portion of our Cpx-Opx tranisition loop above about 950°C (fig. 5A) probably corresponds to the pigeonite-hypersthene transition in natural (Mg-bearing) pyroxenes.

Extrapolation of high-pressure, high-temperature data for the Cpx-Opx inversion of $FeSiO_3$ indicates that there may be a metastable inversion at approximately 900°C at low pressures. This extrapolation has been confirmed in part by unreversed hydrothermal experiments at 100 bars in which OFs inverts to ClFs (in the stability field of fayalite + tridymite) at and above 900°C (table 3).

TABLE 3

Experiments for ferrosilite bulk composition

Starting material ($FeSiO_3$)	Pressure, bars	Temp., °C	Apparatus and remarks*	Time, hours	Results
OFs + ClFs	20,000	760 ± 10	Wet, p. and c.	21	All OFs
OFs + ClFs	20,000	650 ± 10	Wet, p. and c.	92	OFs >> ClFs
OFs + ClFs	20,000	650 ± 10	Dry, p. and c.	92	ClFs
OFs	100	950 ± 5	FMQ, T.p.	0.5	OFs + ClFs + Fay + SiO_2
OFs	100	925 ± 5	FMQ, T.p.	0.8	OFs + minor ClFs + Fay + quartz
OFs	10,000	900 ± 15	Dry, s.s.	0.2	ClFs + magnetite + quartz

*Wet: hydrothermal experiment performed in a sealed silver capsule with 5 percent excess SiO_2 added to saturate the gas with respect to SiO_2. FMQ: standard hydrothermal buffer experiment using fayalite + magnetite + quartz buffer; sample was contained in a sealed $Ag_{80}Pd_{20}$ alloy capsule. p. and c.: piston-and-cylinder device. T.p. Tuttle press (Tuttle, 1948). s.s.: opposed anvil shearing squeezer (Bell and England, 1967). The sample in the dry piston-and-cylinder experiment was dried in vacuo and was contained in an iron capsule with a tightly fitting lid.

EXTRAPOLATION OF 20 KB RESULTS TO LOW PRESSURES

The experiments delimiting the two-pyroxene field shown in figure 5A were conducted at 20 kb so that the $FeSiO_3$-rich pyroxene would be stable, but in order to apply the results to crustal rocks it is necessary to extrapolate them to lower pressures. In this way we can obtain an estimate of the position of the metastable two-pyroxene field at, say, 1 atm. Most

natural orthopyroxenes contain a fairly constant $CaSiO_3$ content of about 3 percent. Our orthoferrosilites in equilibrium with Cpx at 20 kb contain about 5 percent $CaSiO_3$, so it seems likely that any pressure correction for orthoferrosilite will be small. The correction for the effect of pressure on the composition of the coexisting Cpx depends on the following assumptions: (1) the curve for Cpx in figure 5A represents the mutual interference of a Cpx miscibility gap and a Cpx-Opx transition loop; (2) the Cpx miscibility gap is symmetrical about the critical temperature T_c (fig. 5C); (3) the Cpx solid solution is a regular solution. From figure 5A, we have taken $T_c = 870°C$ at 20 kb, for a composition of approximately $Fs_{75}Wo_{25}$ (corresponding to an equimolar mixture of $Ca_{0.50}Fe_{0.50}SiO_3$ and $FeSiO_3$). We obtain the excess molar volume of mixing, 1.4 ± 0.5 Å^3, from the data of Lindsley, Munoz, and Finger (1969). Following the reasoning of Bell and Davis (1969) we have calculated the pressure effect on this critical temperature. The critical temperature at 1 atm is approximately 820°C.

This result can be combined with the estimated temperature of the Cpx-Opx inversion in $FeSiO_3$ at 1 atm (900°C) to yield the probable form of the metastable two-pyroxene relations on the join Hd-Fs at low pressures.

The inversion temperature decreases much more rapidly with decreasing pressure than does the critical temperature, so that the critical temperature is not more than 80°C below the $FeSiO_3$ inversion temperature at low pressures (fig. 6). For this reason it seems likely that the miscibility gap will penetrate through the inversion loop, resulting in a two-Cpx field over a restricted temperature range as shown in figure 6. These relations are metastable and are based largely on extrapolation over a wide pressure range, but we suggest that they provide an approximate metastable terminus for the two-pyroxene field in the pyroxene quadrilateral: above 820°C there is a broad field of Cpx; just below 820°C there is a field of two clinopyroxenes (corresponding to Hd_{ss} + "ferropigeonite"); at still lower temperatures there is a field of Opx + Cpx (hypersthene + Hd_{ss}). In contrast to these *metastable* relations (fig. 6) is curve 1 from figure 3, which marks the limit of *stable* solubility of $FeSiO_3$ in Hd_{ss}.

APPLICATION OF EXPERIMENTAL RESULTS

Our new experimental data on the join Hd-Fs can now be combined with experimental data for other bounding joins and analytical data for natural pyroxenes to provide some insights into subsolidus relations in the pyroxene quadrilateral. These relations can in turn provide information on the crystallization of pyroxenes from magmas. This discussion will ignore the effects of pressure (which are probably small in crustal rocks) and of minor constituents in the pyroxenes (only those pyroxenes for which $CaSiO_3 + MgSiO_3 + FeSiO_3$ total 90 percent or more will be considered).

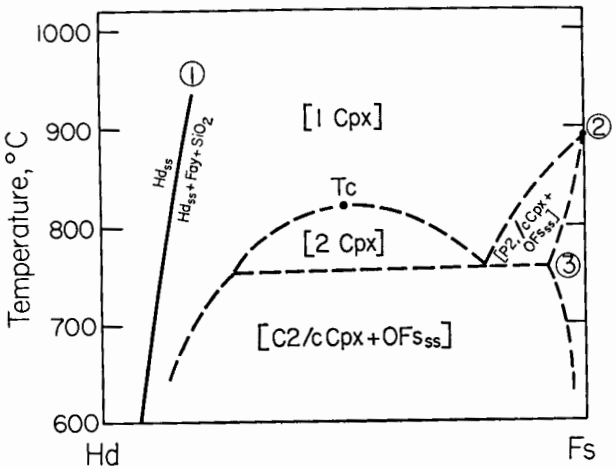

Fig. 6. Suggested hypothetical metastable phase relations for the join Hd-Fs at low pressures (dashed lines) contrasted with a portion of the experimentally determined stable phase relations (solid line). (1): Curve defining the compositions of Hd_{ss} in *stable* equilibrium with Fay + SiO_2 (fig. 3A); (2): *metastable* inversion temperature of OFs $\rightleftharpoons$ ClFs. Unreversed experiments suggest that this inversion lies below 900°C at low pressures; Tc: critical temperature (820°C) of the *metastable* miscibility gap extrapolated from 20 kb experiments; (3); *metastable* 3-phase element $C2/c$ Cpx + $P2_1/c$ Cpx + OFs_{ss} (equivalent to the Mg-bearing assemblage augite + pigeonite + hypersthene). In this interpretation, the miscibility gap has penetrated both limbs of the inversion loop (fig. 5B), and thus there is a three-phase element with a two-Cpx field above it.

At 20 kb the two-pyroxene field evidently extends completely across the quadrilateral at temperatures below 870°C. At low pressures[2] the two-pyroxene field on the Hd-Fs join becomes metastable with respect to the assemblage Hd_{ss} + Fay + SiO_2, so the two-pyroxene field in the quadrilateral must be terminated before the Hd-Fs join is reached. We can estimate the maximum extent of the two-pyroxene field from natural occurrences. Philpotts (1966, p. 28-29) has reported a quartz mangerite that contains an inverted pigeonite with an Fe/Mg ratio (estimated from n_β) of $Fe_{75}Mg_{25}$ and a "Ca-rich" clinopyroxene of composition $Wo_{25.6}En_{22.4}Fs_{52.0}$. This pair of pyroxenes, whose compositions are plotted in figure 7, represents the most iron-rich two-pyroxene assemblage from plutonic igneous rocks known to us, but the two-pyroxene field may in fact extend to still more iron-rich compositions. A fascinating assemblage from an adamellite (Wheeler, 1965) may represent the ultimate limit of the two-pyroxene field in crustal rocks. The adamellite contains a clinopyroxene, $Wo_{36}En_8Fs_{56}$ (optical determination) as well as complex intergrowths of fayalite (Fa_{87} by X-ray), quartz, orthopyroxene (Fs_{84} by optical determination), and lamellae of clinopyroxene. Wheeler interprets these intergrowths as representing initial ferriferous pigeonite which inverted at least in part to orthopyroxene while exsolving lamellae of Ca-rich pyroxene. Subsequently the remaining pigeonite (if any) and much

[2] "Low pressures" in this discussion will refer to pressures of about 2 kb or less.

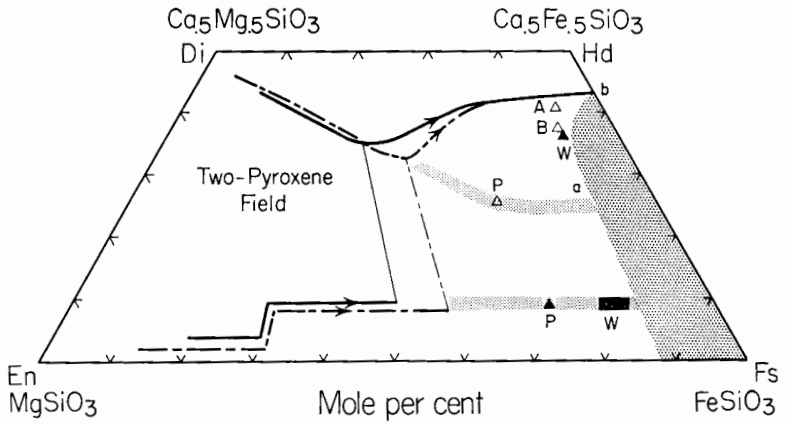

Fig. 7. Suggested polythermal relations in the pyroxene quadrilateral, together with the compositions of some natural pyroxenes. Stippled area: approximate position of "forbidden zone," a three-phase field of the quadrilateral in which no pyroxene is stable at low pressures (from data of Bowen and Schairer, 1935; and this report). The exact boundary of the zone within the quadrilateral is not known but is a function of temperature. For a fixed temperature, the area of the "forbidden zone" will decrease with increasing pressure. Curve a-b: schematic trend of Ca-rich pyroxene compositions in equilibrium with Fay + SiO_2. Solid lines, Skaergaard pyroxene trends; dash-dot lines, Bushveld pyroxene trends. Tie lines link last pairs of Ca-rich and Ca-poor pyroxenes to coexist in each intrusion. Arrows show direction of decreasing temperature. Shaded areas, possible polythermal boundaries of two-pyroxene field for Fe-rich silica-saturated rocks, based on interpolation between the Skaergaard-Bushveld data and our results for the Hd-Fs join. Based on data for the Hd-Fs join, the position of the Ca-rich boundary of this field will be very sensitive to temperature below 820°C. Triangles, pyroxenes from quartz-bearing plutonic rocks. P, coexisting pyroxenes from quartz mangerite, Greenville township, Quebec (Philpotts, 1966, p. 28-29). W (triangle), clinopyroxene from adamellite coexisting with complex intergrowths of fayalite, quartz, orthopyroxene, and lamellae of clinopyroxene; (rectangle), probable bulk composition of the intergrowths. If the Ca-poor intergrowths are interpreted as having crystallized as pigeonite, this represents the most Fe-rich natural two-pyroxene assemblage yet reported (Wheeler, 1965). The width of the two-pyroxene field for this assemblage suggests crystallization at relatively low temperatures. A, clinopyroxene from granophyre, Skye (Anwar, 1955). B, clinopyroxene from another granophyre, Skye (Bell, 1959, cited in Brown and Vincent, 1963). Both A and B coexist with fayalite + quartz. Open symbols, compositions from chemical analysis; closed symbols, compositions from optical data.

of the orthopyroxene decomposed to fayalite + quartz. Evidently this assemblage crystallized at the boundary of a Cpx + Fay + quartz field and entered that field upon cooling. The three-phase field Cpx + Fay + SiO_2 (approximately shown by coarse stippling in fig. 7) is the ultimate terminus for the two-pyroxene field at low pressures. To emphasize the fact that no pyroxene is stable within this three-phase field at low pressures, we have termed it the "forbidden zone" of the pyroxene quadrilateral. The extent of this zone along the Hd-Fs join (fig. 3) is from the Fs apex approximately to $Fs_{60}Wo_{40}$, and its extent along the En-Fs join can be obtained from the data of Bowen and Schairer (1935, p. 164): from the Fs apex approximately to $En_{12}Fs_{88}$ (mole percent) at 950°C and approximately to $En_{40}Fs_{60}$ at 1200°C. A portion of the boundary

within the quadrilateral is given by that tie line between the Ca-rich and Ca-poor pyroxenes that coexist with fayalite + quartz; this too will vary with temperature. We have drawn an estimated boundary (fig. 7) for some temperatures in the range 800° to 950°C. This temperature range probably lies below the solidus for bulk compositions within the quadrilateral (Yoder, Tilley, and Schairer, 1964, p. 129) but may represent crystallization temperatures for some ferriferous magmas.

Points a and b in figure 7 show the compositions of Hd_{ss} in equilibrium with fayalite + quartz in two granophyres from Skye (Anwar, 1955; Bell, 1959, cited in Brown and Vincent, 1963). The bulk compositions of these assemblages lie within the "forbidden zone". The assemblages are similar to those found in the late-stage, quartz-bearing rocks of the Skaergaard and Bushveld intrusions, but the Skye granophyres are believed to have formed, not by fractional crystallization of basaltic magma, but from low-temperature crustal melts (Brown, 1963).

The intersection of the two-pyroxene field with the "forbidden zone" in the presence of liquid corresponds to reaction point "D" at which Cpx, Opx, olivine, tridymite, and liquid coexist (Yoder, Tilley, and Schairer, 1963, p. 87) for bulk compositions lying in the pyroxene quadrilateral. The presence of additional components in magmas will, of course, lower the temperature and therefore also alter the compositions of the phases at which the reaction takes place.

It is clear from figure 7 that the two-pyroxene fields of the Skaergaard and Bushveld trends are terminated well before the "forbidden zone" is reached: Ca-poor pyroxenes cease to crystallize when they have attained Fe/Fe + Mg ratios between 0.50 and 0.58; concomitantly the Ca-rich pyroxenes attain a minimum calcium content, and olivine rejoins the crystallization sequence (fig. 1).

The sequence of crystallization of mafic silicates and quartz as primary (cumulus) minerals in the Skaergaard intrusion is as follows (Wager and Brown, 1968):

IV. Hd_{ss} (or Wo_{ss}) + fayalite + quartz (Upper Zone c).
III. Ca-rich pyroxene + olivine, both with high Fe/Mg ratios (Upper Zone, a, b).
II. Ca-rich + Ca-poor pyroxenes, both with intermediate Fe/Mg ratios (Middle Zone).
I. Ca-rich + Ca-poor pyroxenes + olivine, all with low Fe/Mg ratios (Lower Zone).

Although quartz occurs throughout much of the Skaergaard intrusion, it is clearly an intercumulus mineral except in the latest stages of Upper Zone c (Wager and Brown, 1968, p. 52-54).

Relations of the mafic silicates and quartz in the Bushveld intrusion are not so well known, especially in the later differentiates, but they appear to be grossly comparable with the sequence outlined above for the Skaergaard intrusion. Quartz becomes a primary phase only in the very late-stage ferrodiorites and syenodiorites of the Bushveld intrusion

(Wager and Brown, 1968; G. M. Brown, personal commun., 1968). As in the Skaergaard intrusion, olivine precipitated early, then ceased to crystallize, and finally reappeared concomitantly with the disappearance of Ca-poor pyroxene.

Of vital importance in the discussion that follows is the assumption that the disappearance of primary Ca-poor pyroxene and the concomitant reappearance of primary olivine in the Skaergaard and Bushveld intrusions was *not* accompanied by the precipitation of primary quartz. The evidence in favor of this assumption is good in the case of the Skaergaard intrusion but only fair for the Bushveld intrusion. It is conceivable that the crystallization of primary quartz did accompany the reappearance of olivine, but that the quartz floated and is therefore absent in all but the uppermost parts of the layered series. In the absence of positive evidence to support this hypothesis, however, we shall assume that the primary precipitation of quartz did not accompany the disappearance of Ca-poor pyroxene and the reappearance of olivine in either the Skaergaard or Bushveld intrusions.

So far as the solid phases are concerned, the assemblages Ca-rich pyroxene + Ca-poor pyroxene + liquid and Ca-rich pyroxene + olivine + quartz + liquid are degenerate: the variance of each solid assemblage is indifferent to the presence of liquid. At any given stage in the crystallization of a magma the assemblage Ca-rich pyroxene + Ca-poor pyroxene *defines* the activities (or chemical potentials) of $CaSiO_3$, $MgSiO_3$, and $FeSiO_3$ and restricts the activities of CaO, MgO, FeO, and SiO_2 within fixed but as yet unknown limits; that two-pyroxene assemblage plus olivine or quartz, or the assemblage Ca-rich pyroxene + olivine + quartz, defines the latter activities as well. Obviously, the liquid itself provides the primary control of these parameters; we are only saying that these solid assemblages can potentially provide information that does not require previous knowledge regarding the liquid.

If a magma that is precipitating Ca-poor pyroxene (or olivine + quartz) also precipitates Ca-rich pyroxene of a given Fe/Mg ratio, the calcium content of the latter pyroxene is a function only of temperature (at a given pressure). If, on the other hand, Ca-rich pyroxene is precipitated in the absence of Ca-poor pyroxene (or olivine + quartz), its calcium content can vary at a fixed temperature as a function of certain intensive chemical parameters (listed above) in the liquid. We will show that the activity of silica is a useful and adequate, although by no means unique, expression of these parameters.

It is important to note that the disappearance of Ca-poor pyroxenes in the Skaergaard and Bushveld intrusions is accompanied by reappearance of olivine *without primary quartz* and therefore cannot be caused by a reaction such as

$$\text{Ca-poor pyroxene} + \text{liquid} = \text{Olivine} + \text{quartz}$$

Evidently the activity of silica (a_{SiO_2}) in these magmas was too low to permit *primary* precipitation of quartz at this stage of fractionation.

(That the magmas were *nearly* saturated with respect to SiO_2 is indicated by the crystallization of quartz as an intercumulus mineral.) Accordingly, we can write a reaction that relates the disappearance of Ca-poor pyroxene to the silica activity in the magma rather than to the precipitation of quartz. Because it is the $FeSiO_3$ component that leads to the instability of Ca-poor pyroxene, we may write the reaction thus:

$$\begin{array}{lcll} (Fe_2Si_2O_6)_{ss}{}^3 & = & (Fe_2SiO_4)_{ss} & + & (SiO_2) \\ \text{in pyroxene} & & \text{in olivine} & & \text{in melt} \end{array} \qquad (3)$$

The effect of silica activity in controlling whether an olivine or a Ca-poor pyroxene will crystallize from a magma can be seen from the equilibrium condition:

$$K_3 = \frac{a_{Fe_2SiO_4} \cdot a_{SiO_2}}{a_{Fe_2Si_2O_6}}$$

It is clear that at equilibrium a decrease in the activity of SiO_2 must entail a decrease in the activity of $Fe_2Si_2O_6$ or an increase in the activity of Fe_2SiO_4, or both. The maximum stability of $FeSiO_3$-rich pyroxene will obtain when $a_{SiO_2} = 1$; that is, when the liquid is saturated with respect to SiO_2 and quartz is a primary phase. This corresponds to the intersection of the Ca-poor trend line with the "forbidden zone". At lower values of a_{SiO_2} however, $FeSiO_3$-rich pyroxene will be less stable, and reaction (3) will take place earlier in the differentiation sequence, before the trend-line for Ca-poor pyroxenes reaches the "forbidden zone".

We suggest, therefore, that the disappearance of Ca-poor pyroxene and reappearance of olivine during crystallization of the Skaergaard and Bushveld intrusions are controlled by reaction (3), with $a_{SiO_2} < 1$. We further suggest that the different Fe/Mg ratios of the last Ca-poor pyroxenes in each body reflect—at least in part—a slightly higher value of a_{SiO_2} during the intermediate stages of crystallization in the Bushveld intrusion than during the equivalent stages of the Skaergaard intrusion. Three points are worth emphasizing here: First, the values of a_{SiO_2} in both intrusions were only slightly below unity (quartz was an intercumulus phase during much of the crystallization sequence and was a primary phase in the latest differentiates), and the difference in a_{SiO_2} between the intermediate stages of each intrusion was probably small. Second, the disappearance of Ca-poor pyroxene does not necessarily require that either the percentage *or* activity of silica actually decreased during fractionation of the Skaergaard and Bushveld intrusions; it is only necessary that a_{SiO_2} failed to increase sufficiently to stabilize Ca-poor pyroxenes with high Fe/Mg ratios. Third, the activity of silica is likely to change during fractionation of any magma, and it is strictly

[3] The use of the double formula for the ferrosilite component here serves to emphasize the fact that the Fe^{++} occupies two energetically different sites in the pyroxene structure.

correct to speak of *the* a_{SiO_2} of the magma only at a restricted place and time. Where necessary, we shall use terms such as "range of a_{SiO_2}" to emphasize this fact.

That the foregoing treatment is not trivial can be seen from the following considerations. It will eventually be possible to evaluate the equilibrium constant, K_3, for a variety of temperatures by determining the compositions of Ca-poor pyroxene and of olivine that are in mutual equilibrium with quartz. Under these conditions, $a_{SiO_2} = 1$, and $a_{Fe_2Si_2O_6}$ and $a_{Fe_2SiO_4}$ may be estimated from mole fractions (ultimately this estimate can be improved by the use of appropriate activity coefficients). The evaluation of K_3 in this way is independent of the presence of liquid. If an estimate of crystallization temperature can be made, it will then be possible to determine the range of a_{SiO_2} at which Ca-poor pyroxenes ceased to crystallize in these two intrusions.

We can now present an alternative explanation to that of Yoder, Tilley, and Schairer (1963, p. 87; 1965, p. 121) for the calcium minima in the trend-lines for Ca-rich pyroxenes from the Skaergaard and Bushveld intrusions (figs. 1, 7). Those workers indicated that the calcium minima—and the concomitant disappearance of Ca-poor pyroxene—might mark an invariant reaction point at which Ca-rich pyroxene, Ca-poor pyroxene, olivine, SiO_2 (as quartz or tridymite), and liquid coexist (point "D", 1963, p. 87). According to this interpretation, crystallization took place along a univariant curve such as Cpx + Opx + SiO_2 + liquid before the reaction point was reached and along the curve Cpx + Ol + SiO_2 + liquid thereafter. (In magmas these assemblages are not strictly invariant and univariant, but it is convenient and useful to relate them to a simple model—the pyroxene quadrilateral—where the variance is rigorously correct.) But this reaction point interpretation requires the presence of a primary silica phase, which appears not to be the case in the appropriate portions of the Bushveld and Skaergaard intrusions. Crystallization in the absence of quartz would take place along the equivalent of divariant surfaces Cpx + Opx + liquid before the Ca-rich minimum was reached and Cpx + Ol + liquid thereafter. The crystallization trend must therefore have crossed the univariant curve Cpx + Opx + Ol + liquid. Normally, crystallization would be expected to follow along this univariant curve, with the olivine and both pyroxenes becoming increasingly iron-rich, until the liquid reached reaction point "D".

However, it has already been shown that the disappearance of Ca-poor pyroxenes is a function of a_{SiO_2} in the Skaergaard and Bushveld intrusions. We suggest that the different minima in the trend-lines for Ca-rich pyroxenes (fig. 7) likewise reflect the different values of a_{SiO_2} in these intrusions at which the crystallization path was forced off the Cpx + Opx + Ol + liquid curve. Clearly the point at which the liquid leaves that curve (and therefore the Fe/Fe + Mg ratios of the phases)

depends on the value of the silica activity. Consider two extreme cases: (1) If a_{SiO_2} is high—say, quartz is a primary phase—throughout the crystallization history of some hypothetical magma, then the trend-line for Ca-poor pyroxenes can extend to the boundary of the "forbidden zone". Simultaneously, the trend-line for Ca-rich pyroxene will be constrained to the boundary of the two-pyroxene field until it too intersects the boundary of the "forbidden zone"; thereafter the composition of the Ca-rich pyroxene will move along the boundary of that three-phase field (curve a-b in fig. 7, if the possible appearance of Wo_{ss} is neglected), as fayalite and quartz precipitate in place of Ca-poor pyroxene. This is the case that was considered by Yoder, Tilley, and Schairer. (2) If, on the other hand, the range of a_{SiO_2} is low, as in a critically undersaturated magma, Ca-poor pyroxenes will be absent throughout the primary crystallization history. The trend-line for Ca-rich pyroxenes, therefore, will be nowhere constrained to the boundary of the two-pyroxene field but will lie between that boundary and the Di-Hd join, probably at an approximately constant calcium content.

Magmas with ranges of a_{SiO_2} values intermediate between these two extremes will have intermediate trend-lines for Ca-rich pyroxenes. Early in the crystallization histories of such magmas, Ca-poor pyroxenes will precipitate, and for that same crystallization interval the trend-line for Ca-rich pyroxene will be constrained to the boundary of the two-pyroxene field. But, when crystallization of Ca-poor pyroxene ceases, the composition of Ca-rich pyroxenes must move away from that boundary. It is at this stage that the calcium minimum in the Ca-rich trend-line occurs: the compositions of the Ca-rich pyroxenes must move away from the En-Fs join (because Ca-poor pyroxenes are no longer stable) and toward greater Fe/Mg ratios (because the Fe/Mg ratio of the magma increases with fractionation). The resultant direction of the Ca-rich trend-line is approximately toward Hd. Because the Fe/Mg ratio of the last Ca-poor pyroxene is a function of a_{SiO_2} the Fe/Mg ratio of the calcium minimum likewise depends on that parameter. Thus while the early (Mg-rich) portions of the Ca-rich trend-lines tend to coincide (figs. 1, 7), there will be a family of calcium minima and of the subsequent portions of the Ca-rich trend-lines, depending on the range of a_{SiO_2} in each parental magma. The intermediate portions of the trend-lines for Ca-rich pyroxenes from the Skaergaard and Bushveld intrusions are two established members of this theoretical family of curves. Other factors being equal, the lower the value of a_{SiO_2} in a magma, the lower will be the Fe/Mg ratio at which the trend-line for Ca-poor pyroxene moves away from the boundary of the two-pyroxene field.

The trend-lines for Ca-rich pyroxenes from the Skaergaard and Bushveld intrusions again coincide at high Fe/Mg ratios (figs. 1, 7). According to the analysis presented here, it appears that the values for a_{SiO_2} were similar during the later crystallization stages of both intrusions. This conclusion is not inconsistent with the argument (p. 316) that the

a_{SiO_2} values during the intermediate stages of the Skaergaard intrusion were slightly lower than those in the equivalent interval of the Bushveld intrusion. During that crystallization interval when the residual liquids of each intrusion precipitated Ca-rich pyroxenes with Fe/(Fe + Mg) ratios of 0.43 to 0.53, (that is, in the interval between the tie lines in fig. 7) the Skaergaard liquid precipitated olivine and the Bushveld liquid precipitated Ca-poor pyroxene (fig. 1). Thus, to the extent that the proportions of other phases were similar, the residual liquid of the Skaergaard would have gained silica relative to that of the Bushveld during this crystallization interval. An independent indication that the values of a_{SiO_2} became similar with increasing fractionation is the fact that quartz was a primary phase during the very late crystallization stages of both intrusions.

In this discussion we have been treating a_{SiO_2} as an independent and fundamental parameter. It is, in fact, only a useful and convenient expression of related chemical parameters in the magma that are equally significant: a_{FeO}, a_{MgSiO_3}, et cetera. The activity of silica becomes an especially convenient parameter when applied to magmas that have precipitated quartz. It is worth remembering that a_{SiO_2} is proportional to the percentage of silica in the melt *times* an activity coefficient that is a complex function of the bulk chemistry and structure of the magma. Any technique that provides a measure of a_{SiO_2} in a liquid may therefore provide information on the activity coefficient as well.

Two basic assumptions have underlain this discussion: that the effects of pressure and of minor constituents in the pyroxenes can be ignored. But pressures of about 15 to 17 kb stabilize ferrosilite, and therefore at a given temperature the area of the "forbidden zone" will decrease with increasing pressure. The Labrador adamellite (Wheeler, 1965) and the Skye granophyre (Bell, 1959, cited in Brown and Vincent, 1963) both precipitated Ca-rich pyroxenes of similar compositions (fig. 7); but the adamellite initially precipitated Ca-poor pyroxene as well, whereas the granophyre precipitated fayalite + quartz. It is possible that this difference reflects crystallization of the adamellite under more deep-seated conditions. If so, this may be a rare case where pressure has significantly affected the metasilicate assemblage in crustal rocks. The assumption that the effects of minor constituents on the subsolidus relations of pyroxenes can be ignored must, of course, be subjected to further testing. It is our opinion, however, that temperature and a_{SiO_2} were the dominant controls in the differences and similarities between pyroxenes of the Skaergaard and Bushveld intrusions, rather than pressure or minor constituents.

In summary, in the Skaergaard and Bushveld intrusions, the early assemblage Ca-rich pyroxene + Ca-poor pyroxene and the very late assemblage Ca-rich pyroxene + fayalite + quartz were each effectively divariant: given a bulk Fe/Mg ratio, the composition of each phase was fixed by temperature. During intermediate stages of crystallization, when

Ca-rich pyroxene was precipitated in the absence of either Ca-poor pyroxene or quartz, the calcium content of Ca-rich pyroxene with a given Fe/Mg ratio can vary at a fixed temperature, depending on certain chemical parameters of the magma. The activity of silica is a convenient—although by no means unique—expression of those parameters.

ACKNOWLEDGMENTS

Many of our colleagues have contributed through their stimulating discussions of the ideas contained in this paper, and in particular, F. R. Boyd, G. M. Brown, and H. S. Yoder, Jr., improved the manuscript with constructive criticisms (although we take full responsibility for the interpretations presented). C. G. Hadidiacos assisted us with the microprobe analyses. To them all we express our deep thanks.

APPENDIX

Starting Materials

The starting phases were synthesized from 99.999 percent iron sponge (United Mineral and Chemical Supply Co., lot #16848); Fisher's "Certified" Fe_2O_3, lot #764442; Bakers Analyzed $CaCO_3$, lot #10641; quartz from Lisbon, Md. (assay 99.97 percent SiO_2); and Corning 7940 Silica glass (0.000X Fe, 0.0018 Al, 0.0012 Mg, and 0.0022 Ca). Equimolar amounts of $CaCO_3$ and SiO_2 were fired in air to drive off CO_2; CaO could then be weighed as $CaSiO_3$. Since iron-bearing starting phases were synthesized in containers closed to oxygen, it was essential that iron be added as the bulk composition FeO. Wüstite ($Fe_{1-x}O$) is non-stoichiometric and therefore unsatisfactory. The following technique gave good results: Iron sponge, stored in an evacuated desiccator for more than a year, is observed to attain an essentially constant oxygen content of about 2 wt percent. This oxygen content is calculated as Fe_2O_3; then sufficient Fe_2O_3 is added to yield a bulk composition of FeO. This mixture can then be added to other constituents (SiO_2, $CaSiO_3$) and thoroughly mixed by grinding in an agate mortar under alcohol without appreciable oxidation.

Mixes of $FeSiO_3$ bulk composition, wrapped in silver foil, were crystallized in sealed, evacuated silica-glass tubes at about 900°C to yield equimolar mixtures of fayalite + tridymite, or they were sealed in silver capsules with water and crystallized at 1 kb and 800°C to an equimolar fayalite + quartz assemblage.

Mixes for Ca-Fe metasilicates were packed into cylindrical 99.95 percent iron capsules, 6.35 mm outer diameter and 12.7 mm long; the capsules were sealed with tightly-fitting lids. For bulk compositions close to $Ca_{0.50}Fe_{0.50}SiO_3$ the loaded capsules were then sealed in evacuated silica-glass tubes and held for 10 minutes at about 1350°C (well above the liquidus temperatures determined by Bowen, Schairer, and Posnjak, 1933, p. 213).

Although the silica-glass tubes devitrified rapidly under this treatment and commonly cracked upon cooling, the iron capsules remained bright and unoxidized, indicating that the charges had been isolated effectively from atmospheric oxygen. The glasses formed by this technique, still in the iron capsules and sealed anew in evacuated silica-glass tubes, were then crystallized by holding them for several days at temperatures of 1000° to 1050°C (to form Wo_{88}) or 900° to 940°C (to form Hd_{88}).

Compositions richer in $FeSiO_3$ than about $Fs_{65}Wo_{35}$ required a different treatment. The liquidus temperature increases rapidly toward $FeSiO_3$, and it is not feasible to make glasses by the method outlined above. Furthermore, metasilicate phases in the range $Fs_{65}Wo_{35}$ to Fs_{100} are not stable at 1 atm. These phases were therefore synthesized by solid-solid reactions at pressures of 20 to 22 kb and temperatures of 1100° to 1200°C in a large-volume piston-and-cylinder solid-media device designed to take the 6.35 mm x 12.7 mm capsules. The synthesis reaction proceeds slowly, and as limitations of the apparatus preclude runs of more than 3 to 4 hours in this pressure and temperature range, it was necessary to take each sample through several cycles at the desired pressure and temperature. The sample was ground under alcohol in an agate mortar for ½ to 1 hour between each cycle.

During the synthesis process outlined above, the samples gained oxygen rather frequently, apparently from water released by the dehydration of the talc pressure-

medium at pressure and temperature. The oxygen reacted with the iron crucible to yield FeO and thereby drove the composition of the sample off the metasilicate ratio, the excess FeO reacting with $FeSiO_3$ to form fayalite. As Bowen, Schairer, and Posnjak (1933, p. 213-214) pointed out, the appearance of a small excess of fayalite is a sensitive indicator of contamination of the sample by oxidation. We rejected a disheartening number of samples as starting materials because they contained only metasilicate and fayalite. (The presence of fayalite *plus quartz*, on the other hand, only indicated that the synthesis reaction had failed to go to completion.)

A metasilicate sample was accepted as a single-phase starting material if it contained less than about 1 percent fayalite + quartz by visual estimate. We succeeded in synthesizing suitable single-phase starting materials with the compositions $Fs_{50}Wo_{50}$ (hedenbergite), $Fs_{90}Wo_{10}$, $Fs_{85}Wo_{15}$, $Fs_{75}Wo_{25}$, $Fs_{70}Wo_{30}$, $Fs_{85}Wo_{15}$, $Fs_{20}Wo_{10}$, $Fs_{05}W_{5}$, and Fs_{100}. For most of the compositions both the clinopyroxene and pyroxenoid polymorphs were made. These phases, taken singly or combined with each other or with an equimolar fayalite + tridymite or fayalite + quartz mixture, served as starting materials for the equilibrium experiments.

Experimental techniques

For experiments *in vacuo,* 10 to 20 mg of starting material was packed into a 99.95 percent iron capsule (2.39 mm outer diameter and 3.56 mm long, with tightly-fitting lid) which was then sealed in an evacuated silica-glass tube. The evacuated tube was placed in the hot spot of a platinum-wound resistance furnace, the temperature being measured by a $Pt\text{-}Pt_{90}Rh_{10}$ thermocouple adjacent to the sample. The pressure of each experiment was of course the sum of the partial pressures of the species in the system $CaO\text{-}Fe\text{-}FeO\text{-}SiO_2$, very much less than 1 atm at the temperatures employed.

For hydrothermal experiments at pressures from 200 to 2000 bars, 40 to 80 mg of sample together with 2 to 15 mg of water was sealed in $Ag_{80}Pd_{20}$ tubes 3 mm in diameter and 6 to 15 mm long. Each tube was sealed with water and an appropriate redox buffer (Eugster and Wones, 1962, p. 87-91) in a gold tube 5 mm in diameter and 25 to 35 mm long. At temperatures up to 800°C we used standard cold-seal pressure vessels (Tuttle, 1949); at higher temperatures we employed a Tuttle press ("hot seal" pressure vessel, Tuttle, 1948) because the smaller pressure vessels are cheaper and apparently stronger. Water was the pressure medium in both types of apparatus; temperatures were indicated by sheathed chromel-alumel thermocouples.

Samples for our initial hydrothermal experiments at 20 kb utilized the two-tube technique described for buffered experiments at lower pressures, except that the outer gold capsule was designed to finish as a cylinder 6.35 mm in diameter and 12.7 mm long. The assembly was then placed in the large-volume piston-and-cylinder apparatus. The buffer started as nearly pure fayalite; it oxidized slowly to a fayalite + magnetite + ferrosilite assemblage, the pair fayalite + quartz being unstable at 20 kb. The fO_2 of this buffer must be close to that of the fayalite-magnetite-quartz assemblage at lower pressures. Although we made several successful experiments with this technique the double capsules were difficult to prepare to the precise dimensions required to fit the large-volume piston-and-cylinder apparatus. Moreover, in this apparatus the thermal gradient of the furnace cell results in a temperature difference of 20° to 30°C between the middle and ends of the outer capsule. A much smaller gradient is found across the sample capsule in the standard piston-and-cylinder apparatus (Boyd and England, 1963, p. 313; Boyd, 1962, p. 152-153). We found that pure silver capsules (2.39 mm diameter and 3.56 mm long, with tightly-fitting lids) permitted the experiments to be performed successfully in the smaller apparatus. Because the reactions we investigated are not redox reactions, an external buffer is unnecessary if the sample plus water can be maintained as a closed system. No magnetite was detected in most samples, indicating that oxidation did not take place.

The success of these 20 kb experiments depended critically on the preservation of the water (preferably as a separate vapor phase) in the capsule to facilitate reaction rates. Water was detected in each capsule after the experiment, and the presence of a vapor phase at pressure and temperature is inferred from the presence of minute, colorless balls of glass and of radial crystals with low refractive index and low birefringence in most samples. The identification of this material as silica deposited from a vapor phase upon quenching was strengthened by the observation of small amounts of fayalite dispersed within the charge in experiments where the starting material had been initially of metasilicate ratio. We prevented dissociation of the metasilicate by adding 3 to 5 percent excess silica to each charge, an amount that yielded assemblages bearing a small amount of free quartz but no fayalite. Inasmuch as the reactions

studied are independent of the presence of excess quartz, this technique assured that the pyroxenes formed were not driven off composition by loss of silica to the vapor phase.

The quoted pressure of 20 kb is nominal (that is, the product of the pressure on the ram times the areal ratio of the ram to the piston) and is uncorrected for the effects of friction or of strength of the pressure medium (compare Green, Ringwood, and Major, 1966; Richardson, Bell, and Gilbert, 1968, p. 394). However, the high pressure serves only to ensure that all $FeSiO_3$-bearing pyroxenes will be stable relative to fayalite + quartz, and that the actual value of the pressure is relatively unimportant. Temperature was measured with a $Pt\text{-}Pt_{90}Ph_{10}$ thermocouple 0.020 in. away from the capsule and was not corrected for the effect of pressure on the thermocouple.

Properties and compositions of phases: determinative methods

Hedenbergite solid solutions (Hd_{ss}) form faintly greenish, equant to slightly elongate, subhedral grains; wollastonite solid solution (Wo_{ss}) are similar in appearance but are colorless and, for a given composition, have lower indices of refraction than Hd_{ss}. Fayalite forms subhedral to euhedral grains of high refractive index; its color is usually a deeper green than that of the Hd_{ss}. Both quartz and tridymite form subhedral to euhedral grains; they can be distinguished by refractive index as well as morphology.

In 20 kb hydrothermal experiments, orthopyroxene forms prismatic crystals up to 50 μ in size; in the larger crystals, the pink-green pleochroism of hypersthene is common. Certain orthopyroxenes from high-temperature (above 900°C) experiments show very thin, prismatic overgrowths of clinopyroxene, although no internal lamellae of a second pyroxene phase were ever observed. Clinopyroxene is distinguished from orthopyroxene by its inclined extinction and generally smaller and more equant habit. Polysynthetic twinning in clinopyroxene is not uncommon, especially from higher temperature experiments. Because of these significant differences in optical properties, detection of the two-pyroxene assemblage by optical examination is an easy matter.

We determined compositions of clinopyroxenes in the range $Fs_{55}Wo_{45}$ to $Fs_{85}Wo_{15}$ to a precision of $\pm$ 1 percent by measuring (1) the 221, 310, and 311 reflections relative to the 111 peak of silicon, and (2) the differences $(2\theta_{310} - 2\theta_{221})$ and $(2\theta_{331} - 2\theta_{310})$ for copper $K\alpha$ radiation. Inasmuch as $2\theta_{310}$ varies with composition in a direction opposite from that of $2\theta_{221}$ and $2\theta_{331}$, measurement of these differences yields two estimates of composition without need for an added standard. Cell dimensions of the clinopyroxenes synthesized for this study are given by Lindsley, Munoz, and Finger (1969).

We measured the Ca/Fe ratios of orthopyroxenes with a MAC electron microprobe using pyroxenes of known composition ($Fs_{30}Wo_{20}$ and $Fs_{95}Wo_5$) as standards. Calculation of atomic number, fluorescence, stopping power, and backscatter effects for the standards showed that it was unnecessary to apply these corrections to the Ca and Fe values obtained for the unknowns. We did not always correct for background, but the near identity in composition of the $Fs_{95}Wo_5$ standard and the orthopyroxene unknowns (table 2) made this correction unnecessary. Certain clinopyroxenes whose compositions had been previously measured using our X-ray determinative curves were checked against our probe standards; in all cases the agreement with the X-ray compositions was within $\pm$ 1 mole percent $CaSiO_3$.

We determined compositions of Wo_{ss} by observing the shifts in position of three peaks (as yet unindexed) in the range 29.7° to 31.4° 2θ, copper $K\alpha$ radiation.

The calcium content of olivine (expressed as mole percent larnite, Ca_2SiO_4, La) was estimated by comparing the position of d_{130} against d_{130} for synthetic $Fa_{95}La_5$ and for Fa_{100} (Yoder and Sahama, 1957), assuming a straight-line relationship over this narrow range.

References

Anwar, Y. M., 1955, A clinopyroxene from the granophyre of Meall Dearg, Skye: Geol. Mag. v. 92, p. 367-373.

Atlas, L., 1952, The polymorphism of $MgSiO_3$ and solid-state equilibria in the system $MgSiO_3$-$CaMgSi_2O_6$: Jour. Geology, v. 60, p. 125-147.

Bell, P. M., and Davis, B. T. C., 1969, Melting relations in the system jadeite-diopside at 30 and 40 kilobars: Am. Jour. Sci., v. 267-A, Schairer v., p. 17-32.

Bell, P. M., and England, J. L., 1967, High-pressure experimental techniques, *in* Abelson, P. H., ed., Researches in Geochemistry, v. 2: New York, John Wiley and Sons, 663 p.

Bowen, N. L., and Schairer, J. F., 1935, The system MgO-FeO-SiO_2: Am. Jour. Sci., 5th ser., v. 29, p. 151-217.

Bowen, N. L., Schairer, J. F., and Posnjak, E., 1933, The system CaO-FeO-SiO_2: Am. Jour. Sci., 5th ser., v. 26, p. 193-284.

Boyd, F. R., 1962, Phase equilibria in silicate systems at high pressures and temperatures: Apparatus and selected results, *in* Wentorf, R. H., ed., Modern Very High Pressure Techniques: Washington, Butterworths, p. 151-162.

Boyd, F. R., and England, J. L., 1963, Effect of pressure on the melting of diopside, $CaMgSi_2O_6$, and albite $NaAlSi_3O_8$ in the range up to 50 kilobars: Jour. Geophys. Research, v. 68, p. 311-323.

Boyd, F. R., and Schairer, J. F., 1964, The system $MgSiO_3$-$CaMgSi_2O_6$: Jour. Petrology, v. 5, p. 275-309.

Brown, G. M., 1957, Pyroxenes from the early and middle stages of fractionation of the Skaergaard intrusion, East Greenland: Mineralog. Mag., v. 31, p. 511-543.

———— 1963, Melting relations of Tertiary granitic rocks in Skye and Rhum: Mineralog. Mag., v. 33, p. 533-562.

Brown, G. M., and Vincent, E. A., 1963, Pyroxenes from the late stages of fractionation of the Skaergaard Intrusion, East Greenland: Jour. Petrology, v. 4, p. 175-197.

Burnham, C. W., 1965, Ferrosilite: Carnegie Inst. Washington Year Book 64, p. 202-204.

Davis, B. T. C., and Boyd, F. R., 1966, The join $Mg_2Si_2O_6$-$CaMgSi_2O_6$ at 30 kilobars pressure and its application to pyroxenes from kimberlites: Jour. Geophys. Research, v. 71, p. 3567-3576.

Ernst, W. G., 1966, Synthesis and stability relations of ferrotremolite: Am. Jour. Sci., v. 264, p. 37-65.

Eugster, H. P., and Wones, D. R., 1962, Stability relations of the ferruginous biotite, Annite: Jour. Petrology, v. 3, p. 82-125.

Green, T. H., Ringwood, A. E., and Major, Alan, 1966, Friction effects and pressure calibration in a piston-cylinder apparatus at high pressure and temperature: Jour. Geophys. Research, v. 71, p. 3589-3594.

Hess, H. H., 1949, Chemical composition and optical properties of common clinopyroxenes, Pt. I: Am. Mineralogist, v. 34, p. 621-666.

Kushiro, Ikuo, 1969, The system forsterite-diopside-silica with and without water at high pressures: Am. Jour. Sci., v. 267-A, Schairer v., p. 269-294.

Lindsley, D. H., 1965, Ferrosilite: Carnegie Inst. Washington Year Book 64, p. 148-149.

———— 1967, The join hedenbergite-ferrosilite at high pressures and temperatures: Carnegie Inst. Washington Year Book 65, p. 230-234.

Lindsley, D. H., MacGregor, I. D. and Davis, B. T. C., 1964, Synthesis and stability of ferrosilite: Carnegie Inst. Washington Year Book 63, p. 174-176.

Lindsley, D. H., Munoz, J. L., and Finger, L., 1969, Unit-cell parameters of clinopyroxenes along the join hedenbergite-ferrosilite: Carnegie Inst. Washington Year Book 67, in press.

Munoz, J. L., 1968, Effect of shearing on enstatite polymorphism: Carnegie Inst. Washington Year Book 66, p. 369-370.

Philpotts, A. R., 1966, Origin of the anorthosite-mangerite rocks in southern Quebec: Jour. Petrology, v. 7, p. 1-64.

Richardson, S. W., Bell, P. M., and Gilbert, M. C., 1968, The aluminum silicates: Carnegie Inst. Washington Year Book 66, p. 392-397.

Riecker, R. E., Rooney, T. P., 1967, Deformation and polymorphism of enstatite under shear stress: Geol. Soc. America Bull., v. 78, p. 1045-1054.

Sclar, C. B., Carrison, L. C., and Stewart, O. M., 1968, High-pressure synthesis and stability of hydroxylated orthoenstatite in the system MgO–SiO_2–H_2O [abs.]: Am. Geophys. Union Trans., v. 49, p. 356.

Tilley, C. E., Yoder, H. S., and Schairer, J. F., 1964, New relations on melting of basalts: Carnegie Inst. Washington Year Book 63, p. 92-97.

Tuttle, O. F., 1948, A new hydrothermal quenching apparatus: Am. Jour. Sci., v. 246, p. 628-635.

———— 1949, Two pressure vessels for silicate-water studies: Geol. Soc. America Bull., v. 60, p. 1727-1729.

Wager, L. R., and Brown, G. M., 1968, Layered igneous rocks: London, Oliver and Boyd, 588 p.

Wager, L. R., and Deer, W. A., 1939, Geological investigations in East Greenland, III, Petrology of the Skaergaard intrusion, Kangerdlugsuuq, East Greenland: Medd. om Groenland 105, 355 p.

Wheeler, E. P., 2nd, 1965, Fayalitic olivine in northern Newfoundland-Labrador: Canadian Mineralogist, v. 8, p. 339-346.

Yoder, H. S., and Sahama, Th. G., 1957, Olivine X-ray determinative curve: Am. Mineralogist, v. 42, p. 475-491.

Yoder, H. S., Tilley, C. E., and Schairer, J. F., 1963, Pyroxenes and associated minerals in the crust and mantle: Carnegie Inst. Washington Year Book 62, p. 84-95.

———— 1964, Isothermal sections of the pyroxene quadrilateral: Carnegie Inst. Washington Year Book 63, p. 121-129.